Semiannual Progress Report, Jan.-June, 1980

STUDY OF BOUNDARY-LAYER TRANSITION USING TRANSONIC-CONE PRESTON TUBE DATA

Research Grant Number NSG-2396

Principal Investigators

T. D. Reed and P. M. Moretti

School of Mechanical and Aerospace Engineering

Oklahoma State University

Stillwater, Oklahoma 74078

The NASA Technical Officer for this Grant is:

F. W. Steinle, Jr.

Experimental Investigations Branch, 227-5

NASA Ames Research Center

Moffet Field, California 94035

Semiannual Progress Report, Jan.-June, 1980

STUDY OF BOUNDARY-LAYER TRANSITION USING TRANSONIC-CONE PRESTON TUBE DATA

Research Grant Number NSF-2396

Principal Investigators

T. D. Reed and P. M. Moretti

School of Mechanical and Aerospace Engineering

Oklahoma State University

Stillwater, Oklahoma 74078

The NASA Technical Officer for this Grant is:

F. W. Steinle, Jr.

Experimental Investigations Branch, 227-5

NASA Ames Research Center

Moffet Field, California 94035

ACCOMPLISHMENTS

I. An oral presentation was made on July 23 to Mr. F. W. Steinle and personnel of the Experimental Investigations Branch, NASA Ames. At that time, a review of technical progress was given.

II. As discussed in detail within the accompanying report, a correlation of Preston-tube data with theoretical skin-friction coefficient has been achieved for the subsonic, compressible laminar boundary layers on the AEDC Cone. The recommended correlation has been developed using data from nineteen different wind-tunnel conditions and has an rms error in skin-friction coefficient of less than 5%.

III. The STAN-5 computer program for boundary layer calculations is not sensitive to changes in cone pitch or yaw angles. Thus, if the effect of such angles on the correlation is to be studied, a more sophisticated analysis of three-dimensional, viscous flow will be needed, e.g., McRae, et al. [Ref. 1].

IV. The simplified model for calculating the magnitude of Preston-tube pressures (as a function of boundary-layer profile, local static pressure, and probe geometry and position with respect to the wall) does not appear to be a fruitful approach. Thus a more rigorous analysis will be necessary if this type of sensitivity study is to be physically meaningful.

V. An approach for developing a correlation for the subsonic, turbulent boundary layer and transitional region has been selected. Skin friction and velocity profiles, at the beginning of the turbulent boundary layer, can be estimated by using the correlation of Allen [Ref. 2] in conjunction with the Preston-tube data and the Wu and Lock and STAN-5 computer programs. Once the distribution of turbulent skin-friction and boundary layer profiles are available, a correlation between Preston-tube data and theoretical skin friction can be developed using the same techniques employed for the laminar boundary layer. Skin friction within the transition zone can be easily approximated by employing the empirical

intermittency function of Dharwan and Narasimha [Ref. 3]. Although this intermittency functio, is based on flat-plate measurements, the use of actual Preston-tube measurements to specify the extent of the transition zone will result in a very good approximation for the distribution of C_f through the transition zone.

VI. In the case of laminar boundary layers, there is no need to employ the more sophisticated program of Wilcox and Rubesin. However, this program may still be useful in checking the STAN-5 results for compressible, non-adiabatic turbulent boundary layers. This analysis and option will be relegated to future work.

VII. The supersonic wind-tunnel data cannot be successfully analyzed without a calibration of P_{ref} as a function of Preston-tube position, M_∞ and Re_{ft}. The corresponding calibrations for the flight experiments could conceivably be utilized, but this analysis will also be relegated to future work.

REMAINING TASKS TO BE ACCOMPLISHED

UNDER THIS GRANT

I. The effects of changes in nose bluntness on pressure distribution along the AEDC cone will be investigated.

II. Subsonic Preston-tube data will be used to study and compare the onset and extent of boundary layer transition for the corresponding flight and wind-tunnel flow conditions.

III. Use the flight data to develop a correlation for subsonic laminar boundary layers, with and without heat transfer, and compare the results with the corresponding correlation of the wind-tunnel data. The pressure distribution, measured during flight, will be used to calculate the flow, rather than the theoretical pressures of Wu and Lock.

REFERENCES

1. McRae, D. S., Peake, D. J., and Fisher, D. F.: "A Computational and Experimental Study of High Reynolds Number Viscous/ Inviscid Interaction About a Cone at High Angle of Attack," AIAA Paper No. 80-1422, July, 1980.
2. Allen, J. M.: "Reevaluation of Compressible Flow Preston Tube Calibrations," NASA TM X-3488, February, 1977.
3. Dharwan, S. and Narasimha, R.: "Some Properties of Boundary Layer Flow During Transition from Laminar to Turbulent Motion," JFM, Vol. 3, Pt. 4, 1958, pp. 418-436.
4. Higuchi, H. and Rubesin, M. W.: "Behavior of a Turbulent Boundary Layer Subjected to Sudden Transverse Strain," AIAA Journal, Vol. 17, No. 9, Sept. 1979.

CORRELATION OF THEORETICAL LAMINAR SKIN FRICTION WITH PRESTON-TUBE MEASUREMENTS ON A SUBSONIC CONE

By

AYMAN SAID ABU-MOSTAFA

Bachelor of Science

Cairo University

Faculty of Engineering

Giza, Egypt

1970

Submitted to the Faculty of the
Graduate College of the
Oklahoma State University
in partial fulfillment of
the requirements for
the Degree of
MASTER OF SCIENCE
May 1980

ABSTRACT

The laminar boundary layer on a 10-degree cone in a transonic wind tunnel is studied. The inviscic flow and boundary layer development are simulated by computer programs. The effects of pitch and yaw angles on the boundary layer are examined.

Preston-tube data, taken on the Arnold Engineering Development Center (AEDC) Boundary-Layer-Transition Cone in the NASA Ames 11-ft Transonic Wind Tunnel, has been used to develop a correlation which relates the measurements to theoretical values of laminar skin friction. The recommended correlation is based on a compressible form of the classical law-of-the-wall.

The computer codes successfully simulate the laminar boundary layer for near-zero pitch and yaw angles. However, in cases of significant pitch and/or yaw angles, the flow is three-dimensional and the boundary layer computer code used here cannot provide a satisfactory model.

The skin-friction correlation is thought to be valid for body geometries other than cones. It accounts for variable property and heat transfer effects. The rms deviation between theoretical skin-friction coefficients and the corresponding correlation values is < 5 %. Thus, as perhaps

might be expected, this is a better correlation for compressible laminar flows than has been reported for compressible, turbulent layers. The new correlation can be employed in transonic-wind-tunnel tests to relate Preston-tube surveys along models to distributions of laminar, skin-friction coefficient.

ACKNOWLEDGMENTS

I am most grateful to Dr. Peter M. Moretti, my principal adviser, for giving me the opportunity to work on this project and for his helpful suggestions and advice during the course of this study.

I am greatly indebted to Dr. Troy D. Reed for his continuous supervision and excellent guidance.

I would like also to thank Dr. Lynn R. Ebbesen and the staff of the University Computer Center for their help in the development of the computer programs.

This study was arranged through a NASA Ames University Consortium Interchange NCA2-OR535-701, the financial support of which is greatly acknowledged.

TABLE OF CONTENTS

LIST OF TABLES

LIST OF FIGURES

NOMENCLATURE

C_f Local skin-friction coefficient

c_p Specific heat at constant pressure, = 0.24 Btu/lbm°R for air

C_p Preston-tube pressure coefficient, $=(P_{Pt}-P_w)/(0.5\,\rho_e U^2_e)$

D Characteristic dimension of the probe, in.

D_{eq} Equivalent circular diameter of the probe, in.

f' Blasius velocity ratio, $= u/U_e$

G Gain factor for the pressure transducer, psi/in.

g_c Conversion factor, = 32.174 lbm-ft/lbf-s

h Enthalpy, Btu/lbm

H Pressure head, in.

J Mechanical to thermal energy conversion factor, = 778.2 lbf-ft/Btu

k Non-dimensional normal distance, = 2y/D

L Cone axial length, in.

M Mach number

P Pressure, psi

Pr Prandtl number

q Dynamic pressure, psi

r Recovery factor, or radial distance, in.

R Gas constant, = 53.35 lbf-ft/lbm°R for air

R_D Reynolds number based on D and ν_w, $= U_e D/\nu_w$

Re_{ft} Freestream unit Reynolds number, $= U_\infty/\nu_\infty$

Re_x	Length Reynolds number, $= U_e x/\nu_e$
Re_θ	Momentum-thickness Reynolds number, $= U_e \theta/\nu_w$
T	Temperature, °R
T′	Reference temperature, °R
u	Longitudinal velocity inside boundary layer, ft/s
u_{Pt}	Mean velocity across probe face, ft/s
u*	Shear velocity, $=\sqrt{\tau_w/\rho_w}$
u^+	Normalized velocity for wall-law, $= u/u^*$
U	Velocity outside boundary layer, ft/s
x	Distance along cone surface, ft
X	Body force per unit volume, lbf/ft
x*	Dimensionless independent variable, Eqn. (8.13)
y	Distance normal to cone surface, ft
y*	Dimensionless dependent variable, Eqn. (8.8b)
y^+	Wall Reynolds number, $= y\ u^*/\nu_w$

Subscripts

aw	adiabatic wall
B	Blasius solution
c	for cone flow
e	at edge of boundary layer
eff	effective
eq	equivalent
E	external or outer
I	internal or inner
Pt	Preston-tube
ref	reference
s	shorted

t	total
w	at wall or cone surface
W	for wedge flow
o	wind-off
∞	freestream condition

Greek Letters

α	Angle of attack, deg.
$\bar{\alpha}$	Effective angle of attack, deg.
β	Yaw angle, deg., or pressure gradient parameter
γ	Ratio of specific heats, = 1.4 for air
δ	Cone semi-vertex angle, deg., or boundary layer thickness, ft
δ^*	Displacement thickness of boundary layer, ft
Δ	Deflection or increment
ϵ	Azimuth angle, deg.
η	Blasius non-dimensional normal distance, $= y\sqrt{U_e/2 \times \nu'}$
θ	Momentum thickness of boundary layer, ft
μ	Molecular viscosity, lbf-s/ft
ν	Kinematic viscosity, ft^2/s
ν'	Kinematic viscosity evaluated at the reference temperature, ft^2/s
ρ	Density, lbm/ft
τ	Shear stress, psf
ϕ	Angle between cone axis and resolved yaw vector, deg.
ψ	Stream function, lbm/s
ω	Normalized stream function, Eqn.(6.1)

CHAPTER I

INTRODUCTION

The overall objective of this research is a better understanding of boundary layer transition, as reflected in the capability to relate transition on models in transonic wind tunnels to the corresponding free-flight conditions. The particular objective of the work reported herein is to develop a correlation which relates Preston-tube measurements within a laminar boundary layer on a cone to the corresponding theoretical values of skin friction.

Preston-tube measurements along the surface of a sharp 10-degree cone were obtained in the NASA Ames 11-Ft Transonic Wind Tunnel [1]. The minimum and maximum pressure locations, obtained during a survey along the length of the cone, were interpreted as the onset and end of transition, respectively.

The boundary layer on the slender cone was simulated via the STAN5 computer code [2] which is an extended version of Patankar and Spalding's boundary layer program [3]. The inviscid flow was calculated with Wu and Lock's computer program [4], and the results were used as boundary conditions along the outer edge of the boundary layer. Subroutines were added to this program so that arbitrary combina-

tions of pitch and yaw angles can be input, and the pressure distribution along the ray corresponding to the Preston-tube survey is always generated. In addition, a subroutine was added to the Wu and Lock program to calculate the initial profiles needed for STAN5.

The cone is assumed to be stationary, smooth and sharp-nosed. The probe is assumed to be stable, in contact with the cone surface, and lie totally inside the boundary layer. The flow is assumed to be axi-symmetric, adiabatic, compressible and without body forces. The flow outside the boundary layer is assumed to be inviscid and is calculated based on the cone geometry, i.e., viscous interaction is ignored. The study was restricted to laminar boundary layers on the cone at subsonic speeds.

The effect on the inviscid flow of yaw and pitch angles less than the cone semi-vertex angle is easily calculated with the Wu and Lock program. However, the STAN5 program is a two-dimensional boundary layer code and was found to be relatively insensitive to changes in these angles.

A least-squares curve-fitting program [10] was used to arrive at a simple correlation between skin friction and Preston-tube measurements for the laminar, subsonic boundary layer.

CHAPTER II

OBJECTIVES

The first objective of this study was to calculate the best possible initial profiles, which are required to begin numerical boundary-layer calculations, so that boundary-layer predictions would be uniformly accurate. In an earlier study by Huprikar [5], it was found that different starting profiles resulted in differences in the computed shear stress near the tip of the cone. An example of this is shown in Figure 1.

The second objective was to extend the functions of Wu and Lock's program [4], which calculates the inviscid pressure distribution on sharp cones at transonic Mach numbers, so as to automate calculation of the pressure distribution along a ray corresponding to the Preston-tube survey for non-zero pitch (α) and yaw (β) angles. This information then provides the inviscid boundary conditions for calculation of the boundary layer with STAN5. The third objective was to obtain a correlation for skin-friction coefficient or wall-shear stress in terms of the Preston-tube pressure measurements, so that the Preston tube can be used as a skin-friction measuring device.

The present research focuses on the NASA Ames wind tunnel data taken within laminar boundary layers on the AEDC Transition Cone at subsonic speeds.

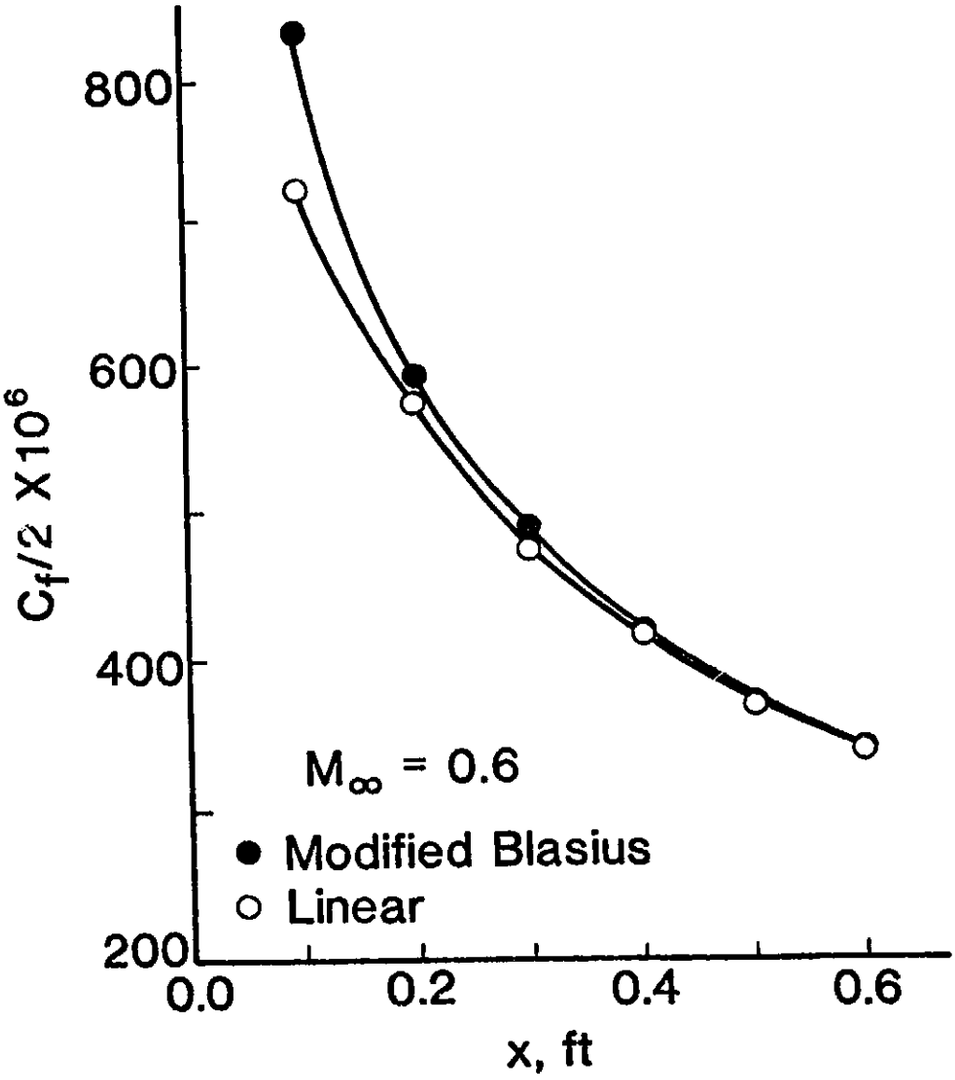

Figure 1. Effect of Initial Profile on Laminar Shear Stress Computation

CHAPTER III

EXPERIMENTAL DATA

3.1 General Background

The measurements utilized in this research were obtained in the NASA 11-Ft Transonic Wind Tunnel at Moffet Field, California. A transonic wind tunnel is an experimental facility intended to simulate the flow over scaled, aerodynamic-test models that would be similar to full-scale venicles during free-flight through the atmosphere at Mach numbers from approximately 0.5 to 1.5.

In transonic flow the difference between the freestream velocity and the speed of sound is small compared to the magnitude of either, and the changes in these parameters are of comparable magnitude. This is contrasted to subsonic flow, where the velocity is lower than the sonic speed and where changes in Mach number are primarily due to changes in freestream velocity at essentially constant sonic speeds, and to supersonic flow where the magnitude of the freestream velocity is substantially larger than the local sonic speec with changes in Mach number occuring through variations of both parameters. In the transonic Mach number range, not only do compressibility effects become important, compared

to lower subsonic Mach numbers where the flow is incompressible, but also the flow at near-sonic speeds is complex because of the mixed type of flow which may exist with local supersonic flow fields contained in subsonic flow regions or local subsonic flow fields embedded in supersonic flow regions. That is why the cone shape is used as a model for boundary-layer-transition research; since it will not have local shocks along the conical surface. At high subsonic speeds, a shock may be generated near the base of the cone owing to flow expansion at the rear of the conical surface and a subsequent recompression in the wake. At supersonic speeds, the cone will, of course, also generate a bow shock, but a shock does not occur on the surface throughout the subsonic Mach number range.

It is worth mentioning that the ventilated, test-section walls of a transonic wind tunnel introduce accustic and streamline disturbances into the test-section flow which means that the wind tunnel flow does not correspond exactly to transonic, free-flight conditions [6]. No satisfactory method has yet been derived to correct for all of the wall effects [7], although this is an area of active research [8].

3.2 Apparatus and Measurements

The experimental data were obtained from a Pitot probe that was traversed longitudinally along the surface of a 5-degree half-angle cone. The cross-section of the opening of the

probe is shown in Figure 2 [9]. The opening has an oval shape with the small dimension normal to the cone surface. The outer height of the probe face is 0.0097", while the centerline of the opening is 0.00453" above the cone surface. A schematic of the experimental model and instrumentation is shown in Figure 3.

The total pressure, as sensed by the Pitot probe, was measured by a differential pressure transducer. The reference pressure for the transducer was taken from the static holes on a flow-angularity probe mounted underneath the cone.

The output from the pressure transducer, ΔH, was recorded, during constant wind tunnel conditions, as a function of x on a plotter. Shorted output of the transducer, for the same wind tunnel conditions, was also plotted on the same plot. The output of the transducer, when the tunnel was off and the transducer was shorted, was also plotted. This output should theoretically be zero. This deflection is called 'wind-off' deflection.

Using this information, the total pressure P_{pt}, as measured by the Pitot probe can be deduced by using the relation

$$P_{Pt} = P_{ref} + G(\Delta H + \Delta H_s + \Delta H_o) \qquad (3.1)$$

Here P ref is the reference static pressure which is considered to be equal to the freestream static pressure [9]. ΔH

is the deflection of the plotter corresponding to the magnitude of ΔP as sensed by the differential pressure transducer. The deflection from the shorted output is ΔH_s, and ΔH_o is the wind-off deflection. G is the gain factor of the plotter, and its value is 0.2515 psi/in. This value was determined from the calibration of the plotter [5].

Twenty-one cases were chosen for detailed analysis. These are all the available, subsonic-wind-tunnel cases with with near-zero flow angles. The tabulated data for these runs is shown in Table I. The freestream Mach number, unit Reynolds number and dynamic pressure are given by M_∞, Re_{ft} and q_∞, respectively, while α and β are the angles of attack and yaw, respectively.

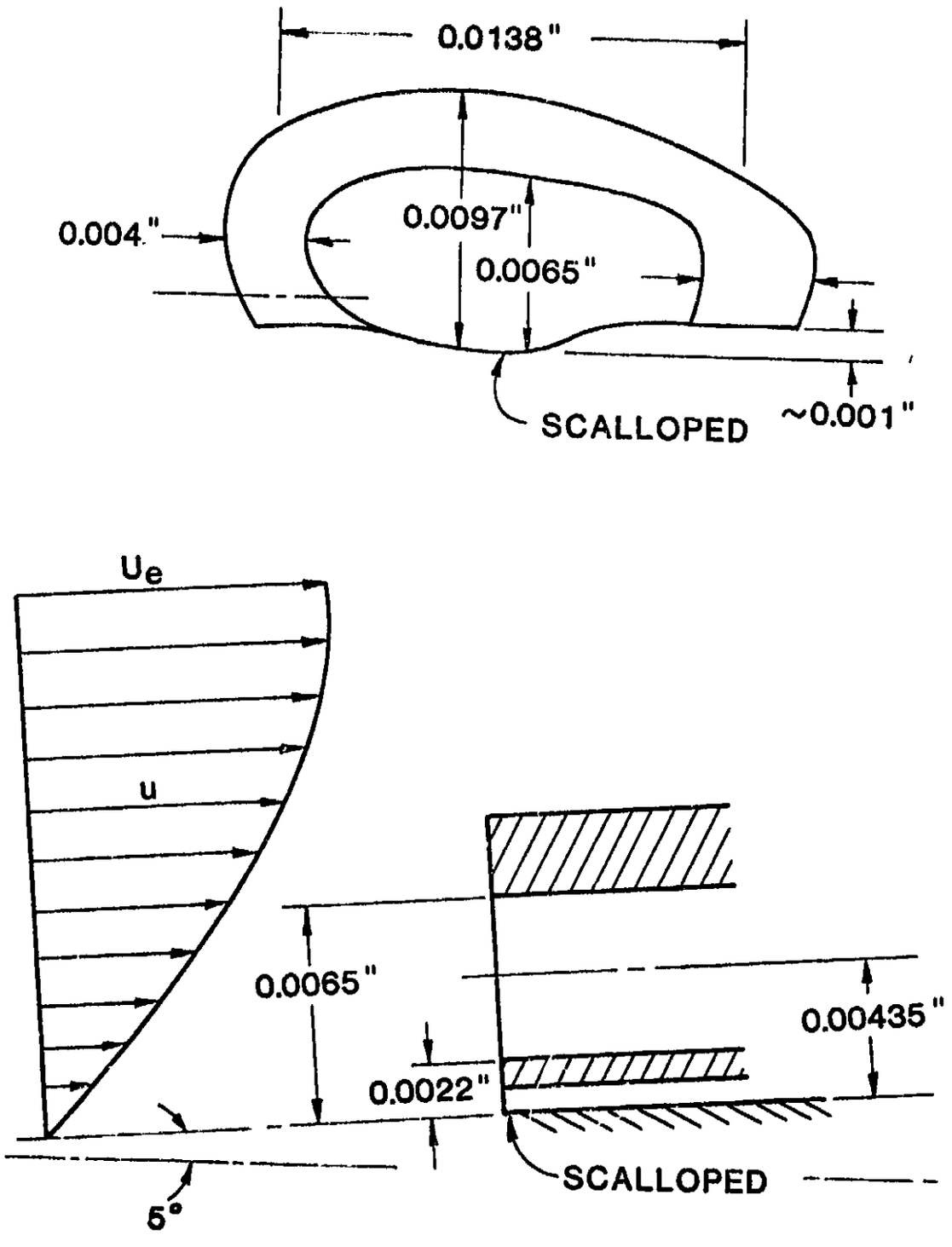

Figure 2. Geometry of the Probe

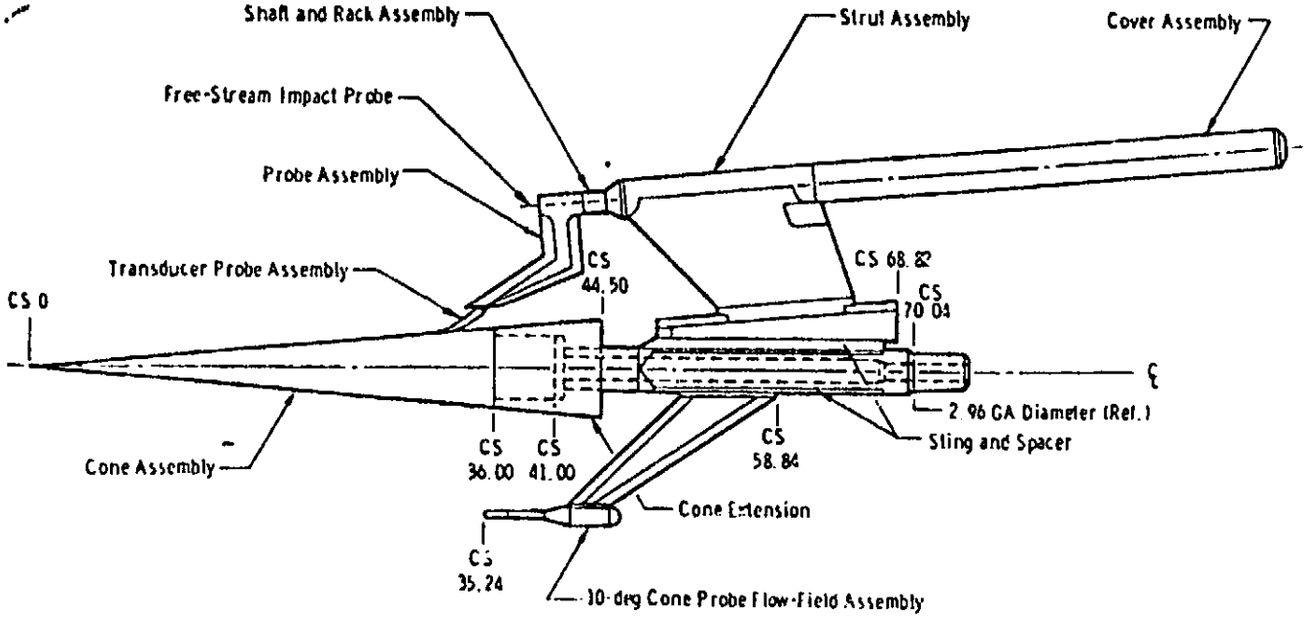

Figure 3. AEDC Transition Cone and Instrumentation

TABLE I

CASES STUDIED

RUN NO.	M_∞	$Re_{ft} \times 10^{-6}$	q_∞	α°	β°
15.231	0.95	4	693	-0.048	0.018
19.289	0.8	4	617	-0.003	-0.022
21.318	0.7	4	548	-0.006	-0.025
23.346	0.6	4	477	-0.001	-0.025
25.376	0.5	4	404	-0.005	-0.025
27.411	0.4	4	403	-0.004	-0.026
29.440	0.3	4	230	-0.006	-0.026
39.545	0.4	2.5	396	0.023	0.021
40.547	0.6	5	586	0.021	0.021
41.548	0.7	5	680	0.018	0.021
42.549	0.8	5	761	0.013	0.021
43.550	0.9	5	842	0.010	0.021
44.551	0.95	5	873	0.008	0.021
56.631	0.9	3	492	0.062	0.006
57.632	0.8	3	453	0.066	0.006
58.633	0.7	3	408	0.071	0.006
59.634	0.6	3	357	0.075	0.006
60.635	0.5	3	302	0.068	0.007
61.636	0.4	3	246	0.070	0.007
70.726	0.7	4	538	0.036	0.023
72.748	0.8	4	605	0.030	0.023

CHAPTER IV

CALCULATION PROCEDURE

The calculation procedure consists of the following steps for each case studied :

1. The given freestream parameters (M_∞ , Re_{ft}, q_∞), as well as the flow angles (α , β), are fed into the extended Wu and Lock program. This program is described in the next chapter and is listed in Appendix F. The output is two-fold:

   a. The inviscid velocity distribution along the cone, and

   b. The initial profiles of velocity and stagnation enthalpy at a distance very close to the tip of the cone.

2. These results are then input to the STAN5 program. A brief description of STAN5 is presented in Chapter VI. The output from that program has detailed information on the boundary-layer properties along the ray of the cone which corresponds to the Preston-tube survey.

When correlation of skin friction was pursued, two more steps were followed :

3. Experimental Preston-tube pressure measurements were calculated from NASA/Ames 11 TWT Preston-tube data [11] using Equation (3.1).

4. These experimental pressures, together with some other parameters* calculated by STANS, were fed into a curve-fitting program [10] to obtain the required correlation. Figure 4 is a flow chart that summarizes the calculation procedure described above.

---

*See Chapter VIII for details.

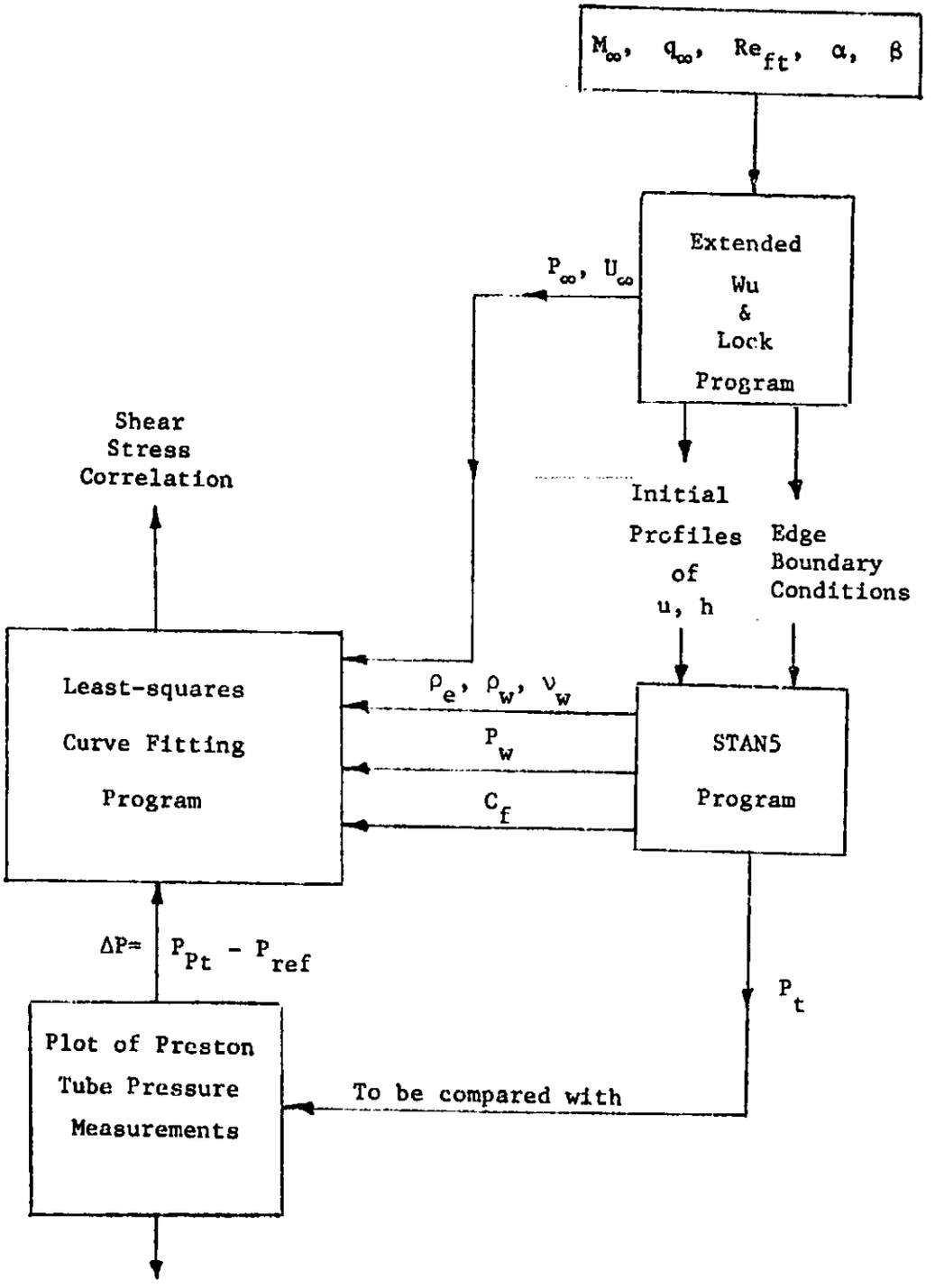

1. Effective center of probe
2. Effect of α, β

. . . etc.

Figure 4. Flow Chart for the Analysis

CHAPTER V

EXTENDED WU AND LOCK COMPUTER PROGRAM

5.1 Introduction

Wu and Lock [4] developed a computer program to calculate the inviscic transonic flow fielc over a sharp-edge smooth cone surface. The program appears to give accurate results [9] when compared with experimental observations. The program, however, handles only yaw angles less than the cone semi-vertex angle. The modified program presented herein calculates the following additional information :

1. The inviscid velocity and pressure distribution along a ray of the cone that corresponds to the Preston-tube survey for arbitrary combinations of α and β,
2. The effect of yaw angles on the inviscic flow field, and
3. The velocity and total enthalpy profiles at a user-specified initial station.

The listing of the extended program can be found in Appendix F. Output for an example run (Case 25.376) is also included.

5.2 The Original Program

The main program reads in M_∞, α, β, and the cone semi-vertex angle δ and and calculates the inviscic-flow pressure

distribution along the cone surface. This is used as the pressure at the edge of the boundary layer. The theory and equations used are described in the Wu and Lock report [4]. The program prints out, along the cone length, the local Mach number M_e and the ratio P_w/P_∞.

5.3 Subroutine ANGLES

This subprogram uses the angle-of-attack α and the yaw angle β to calculate the effective pitch angle $\bar{\alpha}$ and the azimuthal position of the probe ϵ. This subroutine utilizes the equations derived by Dunn et al [11]. These equations are presented in Appendix A. the probe position is considered to be always at the top of the cone and, in accordance with Wu and Lock's notation, $\epsilon = 0.0$ always corresponds to the leeward side of the cone. The calculated angles ($\bar{\alpha}$ and ϵ) are then used in the main program to calculate the inviscid pressure distribution along the top of the cone.

5.4 Subroutine DIST

This subroutine reads in the freestream dynamic pressure (QINF), unit Reynolds number (RLFT) and Mach number (MINF). It then uses these values to calculate the freestream properties (PINF,TINF,RHOINF,MUINF) as well as the total temperature and pressure (TTOT,PTOT). The equations used are the equation of state for a perfect gas (air), Sutherland's equation of viscosity and the isentropic relations [12]. The

details of the calculations are described in Appendix B.

Next, the subroutine uses the local Mach numbers at stations along the cone surface, which are calculated in the main program, to calculate the local temperatures and velocities using isentropic relations. These velocities are then used as the outer boundary conditions for calculation of the boundary layer using STAN5.

5.5 Subroutine INITIA

This last subprogram calculates the velocity and stagnation enthalpy profiles across the boundary layer at a specified initial location. It calculates the average static temperature and viscosity across the boundary layer and uses them to modify the flat-plate Blasius solution so as to apply to the cone problem. The details are presented in Appendix C.

5.6 Checking Wu and Lock Calculations

As a check on the reliability of our version of Wu and Lock's program, the inviscid flow was calculated for a 10-degree cone at a 2-degree pitch angle and compared with those in Wu and Lock's report [4]. The following observations were made :

a. Static pressures on the windward side of the cone are larger than those on the leeward side.

b. Increasing α increases the static pressure on the windward side and decreases it on the leeward side.

c. The slope of the pressure distribution is essentially

the same on both the windward and leeward sides of the cone. (except near the tip and the rear ends of the cone). These checks are shown in Figure 5.

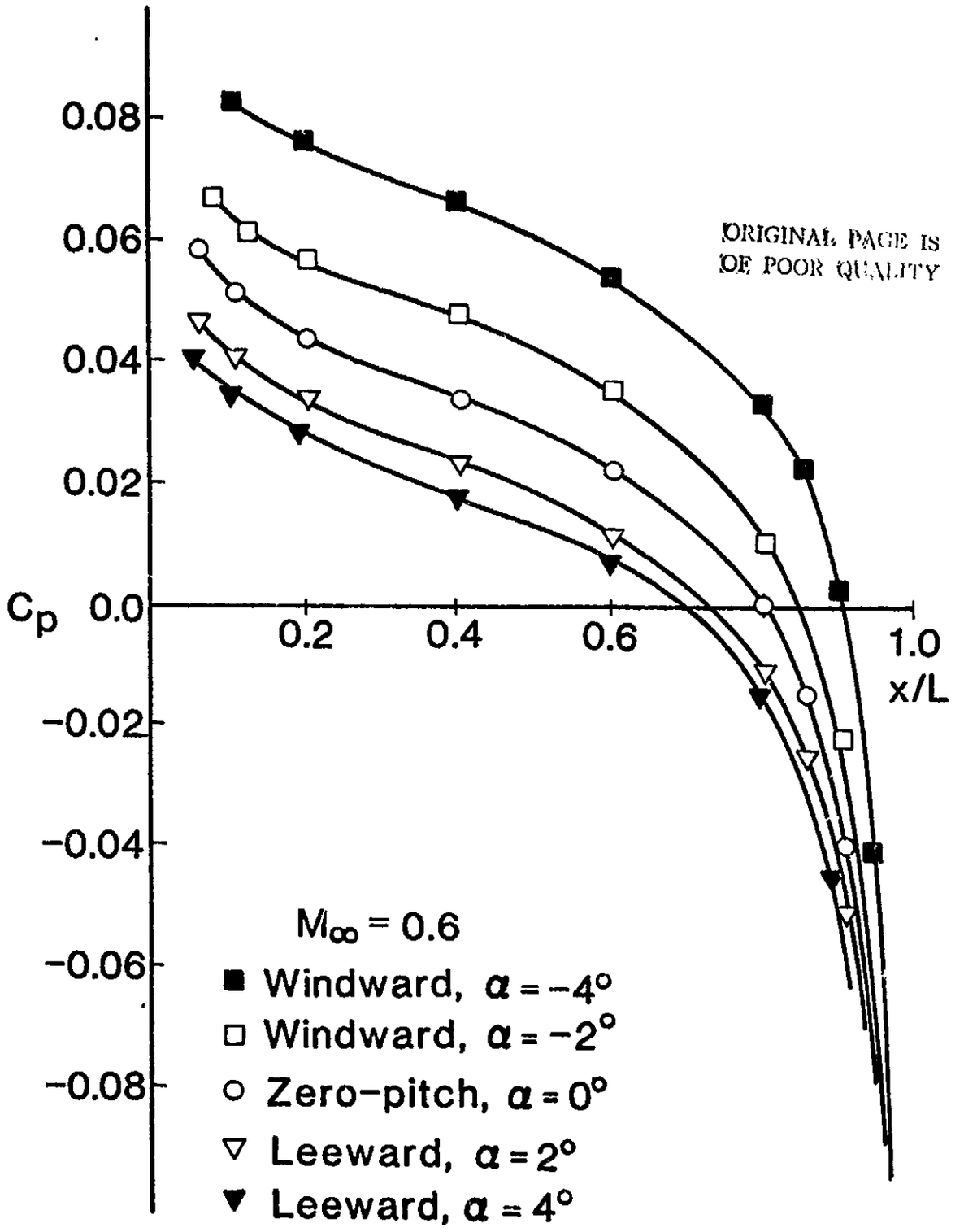

Figure 5. Calculated Pressure Coefficient on Cone Surface for Various Pitch Angles

CHAPTER VI

STAN5 COMPUTER PROGRAM

Based on the work of Patankar and Spalding [3], the STAN5 code was developed by Crawford and Kays [2] as an implicit, finite-difference, forward-marching integration procedure which may be used for computer simulation of boundary layers with transition. The program solves simultaneously equations for conservation of mass, momentum, stagnation enthalpy and up to five mass transfer equations.

The program uses either two-dimensional planar or axi-symmetric type of coordinates so that it is possible to solve for a large variety of flows by simple manipulation of variables. This is accomplished by replacing the y-coordinate with the stream function ψ. The u-velocity component is defined by

$$u = \frac{1}{\rho r} \frac{\partial \psi}{\partial y}$$

and the momentum and energy equations become

$$\rho u \frac{\partial \psi}{\partial x} + \rho u \frac{\partial}{\partial \psi} \left[r^2 \rho u \mu_{eff} \frac{\partial u}{\partial \psi} \right] = -g_c \frac{dP}{dx} + g_c X,$$

and $$\rho u \frac{\partial h_t}{\partial x} + u \frac{\partial}{\partial \psi} \left[r^2 \rho u \frac{\mu_{eff}}{Pr_{eff}} \frac{\partial h_t}{\partial \psi} \right]$$

$$\frac{\partial}{\partial \psi} \left[\frac{\mu_{eff}}{g_c J} \left(1 - \frac{1}{Pr_{eff}} \right) r^2 \rho u \frac{\partial}{\partial \psi} \left(\frac{u^2}{2} \right) \right]$$

The stream function ψ is then normalized by using the transformation

$$\omega = \frac{\psi - \psi_I}{\psi_E - \psi_I} \tag{6.1}$$

where ψ_E and ψ_I are the stream function values on the boundary surfaces or boundary conditions.

A micro-integral method is used to obtain implicit finite-difference equations, which model the partial differential equations and may be used in a downstream, forward-marching solution scheme. The program solves laminar and turbulent boundary layers. Boundary-layer transition is based on the momentum-thickness Reynolds number criterion, which is defined a priori. The way the transition Reynolds number (RETRAN) is specified is as follows :
A very large value is assigned to RETRAN, e.g. 10000, so that the program is ensured to run wholly laminar. From the experimental data sheets obtained from NASA [1], the location of the minimum pressure is considered to be the onset of transition. At this location the corresponding value of Re_θ in STAN5 output is then considered to be the correct RETRAN.

However, since we are presently concentrating only on the laminar boundary layer, a large value of RETRAN was always assigned in the input to STAN5 and no re-run was necessary.

Other input parameters and "flags" are required, a detailed description of which can be found in the STAN5 report [2]. The edge velocity distribution and initial profiles for the velocity and total enthalpy across the boundary layer are required input for STAN5. They are prepared by the extended Wu and Lock program. (See Chapter V).

The output of the program gives, at every incremental x, all the boundary-layer properties of interest, e.g., $u(y), u^+(y), y^+(y), C_f, \delta, \delta^*, \theta, Re_\theta, P_w, T(y), T_t(y), P_t(y), \ldots$ etc. This information can then be used for theoretical analysis of the boundary layer.

CHAPTER VII

EFFECT OF FLOW ANGLES ON BOUNDARY-LAYER CALCULATIONS

As mentioned before in Chapter V, the angles of the freestream flow will affect the boundary-layer flow.* One of the objectives of this research was to investigate the capability of the available computer programs (Wu and Lock's and STAN5) to handle pitch and yaw angles that are a significant fraction of and to obtain some conclusions regarding the analytical tools needed to analyze such cases.

The original Wu and Lock program was modified to calculate the effective yaw angle for arbitrary combirations of yaw and pitch angles. The equations derived by Dunn et al [11] were used in subroutine ANGLES to calculate the azimuth angle of the probe, as discussed in Chapter V. It was found that the extended Wu and Lock program works well with all the cases studied.

One case was studied in some detail, viz., Case 40.547 which has the following data :

$$M_\infty = 0.6,\ Re_{ft} = 5 \times 10^6,\ q_\infty = 586 \text{ psi},$$

$$\alpha = \beta = 0.021^\circ.$$

---

*Transition is affected when α / δ is changed by $\pm 5\%$. (Reference 9).

This case was picked up as a start because of its relatively small Mach number would allow neglection of noise effect [14],[15]. The output of the program (edge velocities and initial profiles) was input to STAN5. It was found that the results of STAN5 for this case were exactly the same as the case of zero flow angles. This was not unexpected since (α) and (β) are very small in this case.

Then, the same case was repeated but with larger angles, viz., α=2.0, β=2.0 degrees, which places the probe 135° from the windward element, and α=-2.0, β=2.0 degrees which places the probe 45° from the windward element. The results of these two runs, together with the original run, are shown in Figure 6. k is defined as 2y/D. The plotted results agree with the observation that the pressures on the windward side are greater than those on the leeward side and that a zero-incidence flow lies in between these. However, by comparing the values of wall shear stress, at the probe azimuth angle, and the boundary-layer thicknesses δ, δ^*, θ, the effect of α and β is negligible as shown in table II. It was, therefore, decided to confine the present stage of research to the cases of very small flow angles. A possible reason for STAN5's insensitivity is its assumption of axisymmetry while real flow with large pitch and/or yaw angles will have significant cross flow, thus forming a three-dimensional flow.

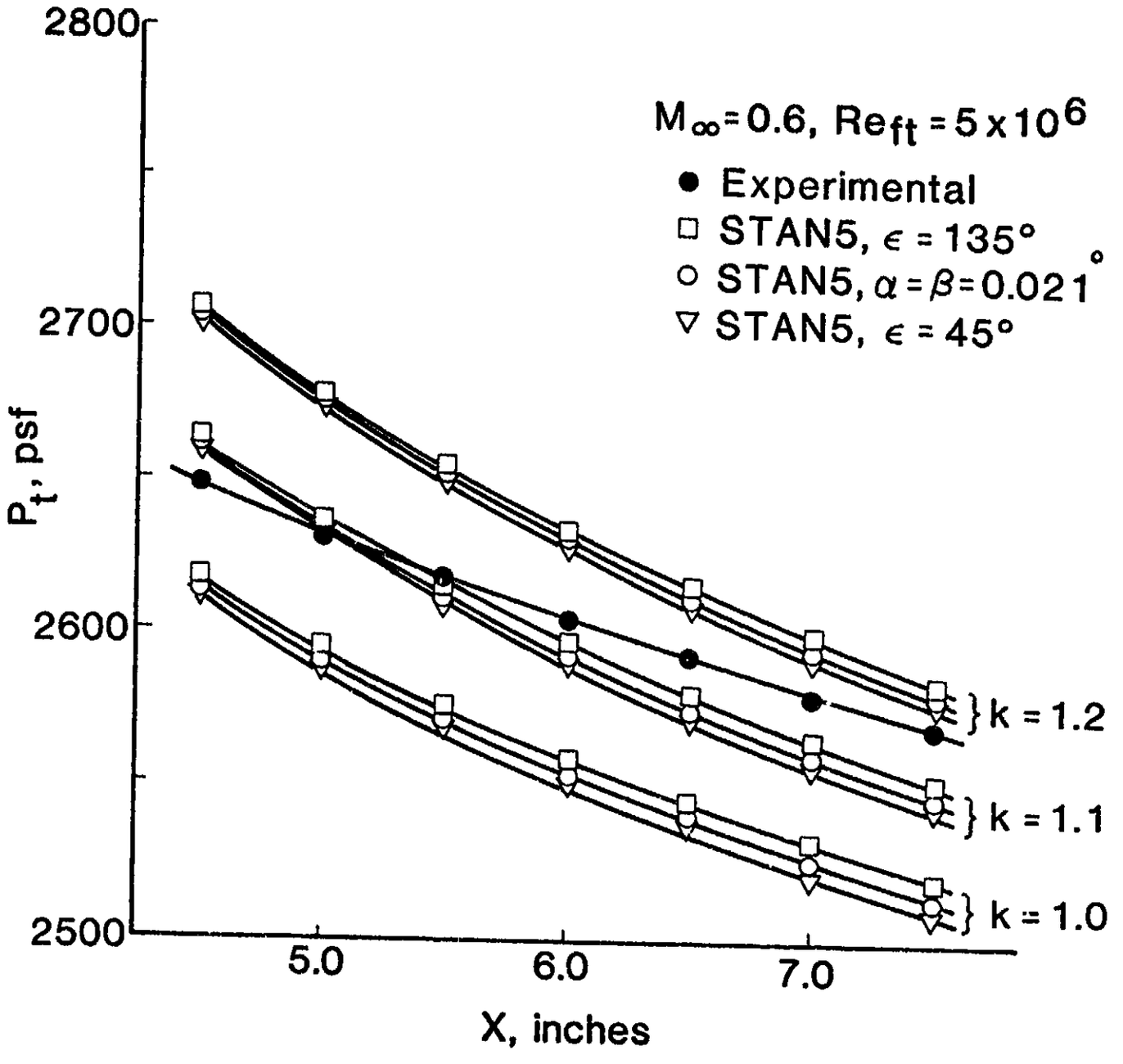

Figure 6. Theoretical Effects of Flow Angles on Effective Pressure at Difierent Heights in the Boundary Layer

TABLE II

SENSITIVITY OF STAN5 COMPUTATIONS TO CHANGES IN FLOW ANGLES[a]

x,ft	$\alpha = \beta = 0.021°$				$\alpha = \beta = 2.0°$ $\varepsilon = 135°$				$\alpha = -2.0°$, $\beta = 2.0°$ $\varepsilon = 45°$			
	$C_f/2$	δ	δ^*	θ	$C_f/2$	δ	δ^*	θ	$C_f/2$	δ	δ^*	θ
0.1	842	615	153	56	838	572	153	56	843	574	153	56
0.2	593	811	216	78	590	849	216	78	593	853	217	78
0.3	483	999	265	95	482	1020	264	95	484	1025	265	96
0.4	417	1157	305	110	417	1182	305	110	419	1188	306	110
0.5	374	1310	341	123	372	1322	341	122	375	1330	342	123
0.6	341	1449	374	134	340	1425	374	134	342	1430	374	134

[a]All numbers, except x, are multiplied by 10^6. The case analyzed is 40.547. The azimuthal angle, ε, corresponds to the probe located at the top of the cone.

CHAPTER VIII

CORRELATION OF SKIN FRICTION

8.1 Theoretical Background

Dimensional analysis [17] has led to a wall-law of the form

$$u^+ = f(y^+) \tag{8.1}$$

where $u^+ = u/u^*$, $y^+ = u^* y/\nu$ and

u=longitudinal velocity, u^*=shear velocity $=\sqrt{\tau_w/\rho}$

If we use the incompressible Bernoulli equation to relate u to the pressure difference between a Preston tube resting on the wall and local static pressure, the law-of-the-wall can then be written in the following form.

$$u_{Pt} = \sqrt{2(P_{Pt} - P_w)/\rho} \quad = \sqrt{2\ P/\rho} \tag{8.2}$$

$$\frac{\sqrt{2\ \Delta P/\rho}}{\sqrt{\tau_w/\rho}} = f\left(\frac{u^*\ y_{eff}}{\nu}\right) \tag{8.3}$$

Now, if we further assume that the effective center of the probe, y_{eff}, is at its half-height, i.e., $k_{eff} = 2y_{eff}/D = 1.0$, then

$$\frac{\Delta P}{\tau_w} = g\left(\frac{u^* D}{2\nu}\right) = g\left(\sqrt{\tau_w D^2/4\rho\ \nu^2}\right) \tag{8.4}$$

Now multiply the numerator and denominator on the left by the appropriate factor, in order to obtain the same grouping of terms as appear in the function g.

$$\frac{\Delta P\ D^2/4\rho\nu^2}{\tau_w D^2/4\rho P^2} = g\left(\sqrt{\tau_w D^2/4\rho\nu^2}\right)$$

or

$$\frac{\tau_w D^2}{4\rho \nu^2} = F\left(\frac{\Delta P D^2}{4\rho \nu^2}\right) \tag{8.5}$$

This last relation provides a convenient way for determining the skin friction since the shear stress is now uniquely related to the difference in pressure head measured with a Preston-tube static-hole combination. For a Preston tube of given geometry, the function F can theoretically be determined from pipe flow experiments where the skin friction can be deduced from measurements of pressure drop. In view of the fact that the wall-laws for pipe and boundary layer flows are identical [17], the calibration is expected to hold also in boundary layer flows.

Equation (8.5) is for incompressible flow in which the assumption of constart properties is valid. For our case, the flow is compressible and the properties, therefore, are not constant. For applications to Preston-tube data, the properties in Equation (8.5) should be evaluated at the wall (cone surface) [13], i.e.,

$$\frac{\tau_w D^2}{4 \rho_w \nu_w^2} = F\left(\frac{\Delta P D^2}{4 \rho_w \nu_w^2}\right) \tag{8.6}$$

The choice of wall properties is consistent with Bradshaw and Unsworth's correlation [20] for compressible, turbulent boundary layer.

8.2 Choice of the Function F

Patel [16],[17] established calibration curves for the laminar sublayer, buffer or transition region and

fully-turbulent layers. His correlation for the laminar sublayer is

$$y^* = 0.5\, x^* + 0.037 \qquad (8.7)$$

where x and y are defined, for compressible flow, as follows:

$$x^* \equiv \log_{10} \frac{\Delta P\, D^2}{4\rho_w \nu_w^2} \qquad (8.8a)$$

$$y^* \equiv \log_{10} \frac{\tau_w\, D^2}{4\rho_w \nu_w^2} \qquad (8.8b)$$

Alternatively, x^* and y^* can be expressed in the form

$$x^* = \log_{10}\left[\frac{C_p}{8}\,\frac{\rho_e}{\rho_w}\,R_D^2\right] , \qquad (8.8c)$$

$$y^* = \log_{10}\left[\frac{C_f}{8}\,\frac{\rho_e}{\rho_w}\,R_D^2\right] . \qquad (8.8d)$$

where C_p = Preston-tube pressure coefficient $= (P_{Pt} - P_w)/(.5\,\rho_e U_e^2)$,

C_f = local skin friction coefficient $= \tau_w/(.5\,\rho_e U_e^2)$, and

R_D = Preston-tube Reynolds number

It was decided to try a straight-line[1] correlation for laminar boundary layers in analogy with Equation (8.7), since it was expected that the behaviour of a laminar sublayer is similar to that of the laminar boundary layer.

---

[1] Later investigation showed that using a second-order function did not improve the curve-fitting accuracy.

8.3 The Curve-Fitting Program

The computer program utilized for the curve fitting is called CURFIT. After applying Equation (3.1), the Preston-tube pressure data is read in, together with other parameters like P_w, C_f, ρ_w, ν_w, and U_e obtained from the Wu and Lock [4] and the STAN5 [2] computer programs.

The probe characteristic length, D, was first taken to be equal to the height of the probe, i.e., 0.0097" (See Figure 2). But since Patel's correlations were based on round probes, it was decided to use an equivalent diameter of the probe. This was done by assuming the probe face to be an ellipse with major and minor axes

$$2a = 0.0138 + 0.004 = 0.0178" \text{ and}$$

$$2b = 0.0097", \text{ respectively.}$$

Then the equivalent circle has an area of

$$\frac{\pi}{4} D_{eq}^2 = \pi ab$$

$$\therefore D_{eq} = \sqrt{4ab}$$

$$D_{eq} = 0.01314"$$

The program then calculates x^* and y^* for each observation point*, and via a curve-fitting package prepared by Dr. Chandler [10] at Oklahoma State University, it fits the values of x^* and y^* to a straight line of the form

$$y^* = Ax^* + K \qquad (8.9)$$

---

*Observation points were taken 0.5" apart down to the end of the laminar portion of the boundary layer.

where A (slope) and F (y-intercept) are constants to be determined by the program.

8.4 Results and Improvements

The resulting straight-line fit to all points was found to be

$$y^* = 0.632\, x^* + 0.415 \qquad (8.10)$$

with a root-mean-square error[a] of 1.2%. This error was considered unsatisfactory.

It was assumed that the reason for this data scatter is the correlation model (8.9) does not account for variable property effects. These effects can be accounted for by introducing the reference temperature, T^*, into the correlation. At this temperature, average values for density and viscosity can be calculated. Tetervin [18] suggested that to transfer the incompressible skin-friction relation of Ludwig and Tillman [19] into compressible form, two parameters need to be included, namely M_e and T^*/T_e. He and numerous other investigators have modeled the effects of these two parameters by introducing density and viscosity at a reference temperature. Although Allen [20] selected the reference temperature of Sommer and Short [13], we have chosen to use Eckert's formula for T' as defined in Equation (C.3). Also,

---

[a] defined as

$$\left\{ \frac{\sum_{\text{all points}} \left(\frac{y^*_{STAN5} - y^*_{CURFIT}}{y^*_{STAN5}} \right)^2}{\text{No. of points}} \right\}^{1/2}$$

the use of the incompressible Bernoulli equation to calculate u_{Pt}, Equation (8.2), is not accurate. Assuming isoenergetic flow ($T_{t,Pt}=T_{t,e}$) across the boundary layer. u_{Pt} can be calculated more accurately as follows:

$$P_{Pt}/P_w = \left(1 + \frac{\gamma-1}{2} M_{Pt}^2\right)^{\gamma/(\gamma-1)}$$

$$\text{or } M_{Pt}^2 = \frac{2}{\gamma-1}\left[(P_{Pt}/P_w)^{(\gamma-1)/\gamma} - 1\right] \tag{8.11}$$

$$\text{and } u_{Pt}/U_e = \frac{M_{Pt}}{M_e}\sqrt{\frac{T_{Pt}}{T_e}} = \frac{M_{Pt}}{M_e}\sqrt{\frac{T_{Pt}}{T_{t,Pt}}}\sqrt{\frac{T_{t,e}}{T_e}}\sqrt{\frac{T_{t,Pt}}{T_{t,e}}}$$

$$\therefore u_{Pt}/U_e = \frac{M_{Pt}}{M_e}\left(\frac{1 + \frac{\gamma-1}{2} M_e^2}{1 + \frac{\gamma-1}{2} M_{Pt}^2}\right)^{1/2} \tag{8.12}$$

and x^* is now defined as

$$x^* \equiv \log_{10}\left(u_{Pt}^2 D^2/4\,\nu_w^2\right) \tag{8.13}$$

Thus, the improved model is in the form

$$y^* = A\,x^* + B\log(T'/T_e) + K$$

The resulting correlation is

$$y^* = 0.655\,x^* + 2.095\log_{10}(T'/T_e) - 0.895 \tag{8.14}$$

with an rms error of 1%. To further improve the fitting accuracy, a quadratic model of the form

$$y^* = A\,x^{*2} + B\,x^* + C\log_{10}(T'/T_e) + K$$

was tried. The result is

$$y^* = 0.273\,x^{*2} - 2.618\,x^* + 1.645\log_{10}(T'/T_e) + 8.921 \tag{8.15}$$

with an rms error of 0.85%. Equation (8.15) can be written in the form

$$C_f = 6.67 \times 10^9 \frac{\rho_w}{\rho_e}\, 10^{+\log_{10}^2(u_{Pt}D/2\nu_w)^{0.546}} \left(\frac{U_{Pt}D}{2\nu_w}\right)^{-5.236} \left(\frac{T'}{T_e}\right)^{1.645} R_D^{-2} \tag{8.16}$$

which has an rms error of 5.85%. Figure 7 shows the data scatter in of C_f. Figure 8 compares the recommended correla-

tion (8.15) with the data. The term z^* is defined as

$$z^* = 0.273\ x^{*2} - 2.618\ x^* + 1.645 \log_{10}(T'/T_e)$$

The extraneous data, which appears above the 10% line in Figure 7, corresponds to a Mach number of 0.80 and Re_{ft} of three and four million. It is speculated that these data are a result of the formation of a transonic shock on the stem of the flow-angularity probe (e.g. see Reference 8) which affects the measured values of P_{ref} and thus P_{Pt}. Discarding only this particular data, a new fit results in the following equation.

$$\boxed{y^* = 0.0942\ x^{*2} - 0.438\ x^* + 2.023 \log_{10}(T'/T_e) + 2.272} \qquad (8.17)$$

The corresponding rms error in C_f is 4.93%. Thus, Equation (8.17) is the recommended correlation for relating C_f and P_{Pt} within subsonic, compressible laminar boundary layers.

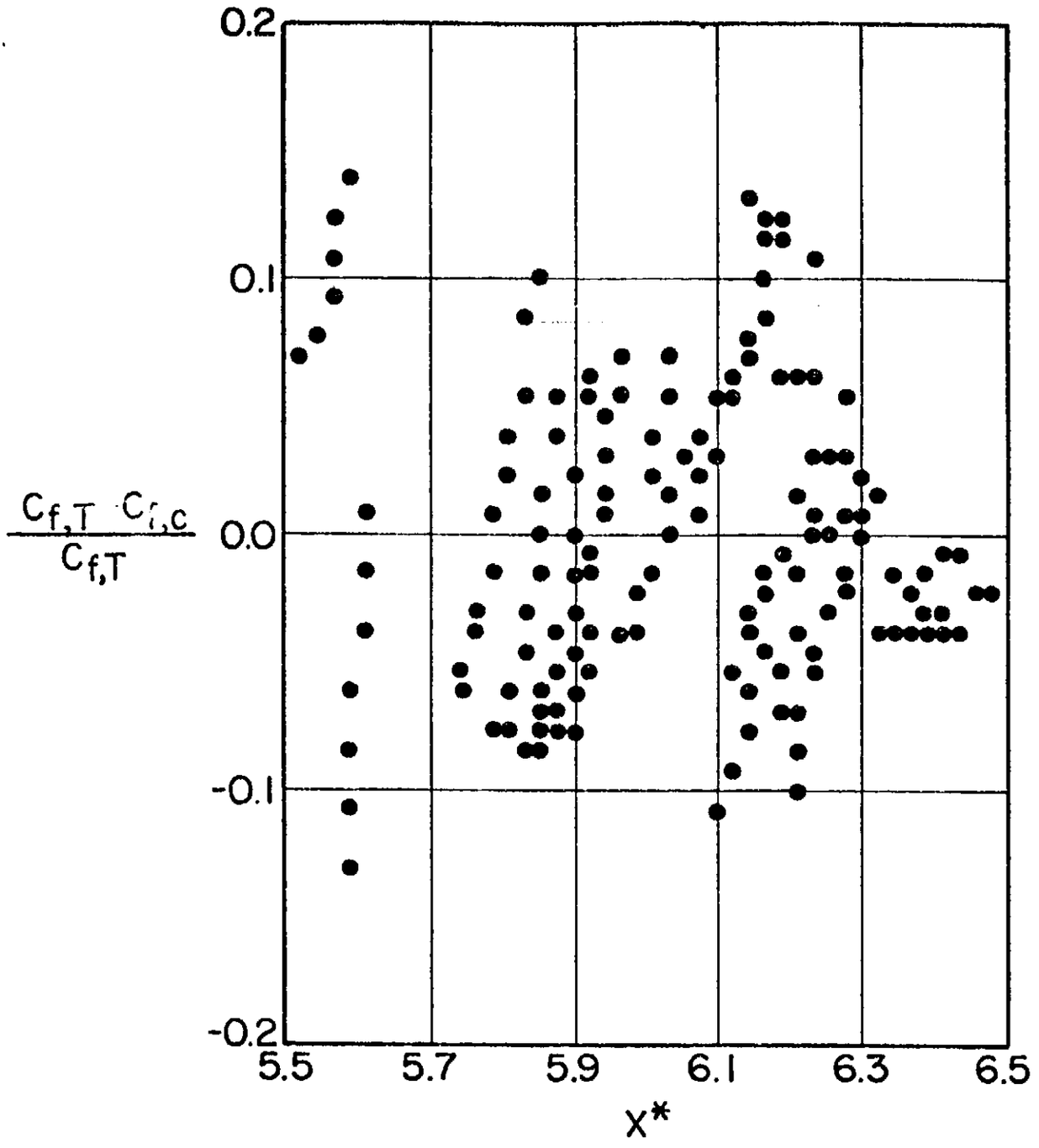

Figure 7. Deviation of Predicted Skin-Friction Coefficient by Eqn. (8.15) from Theoretical Values

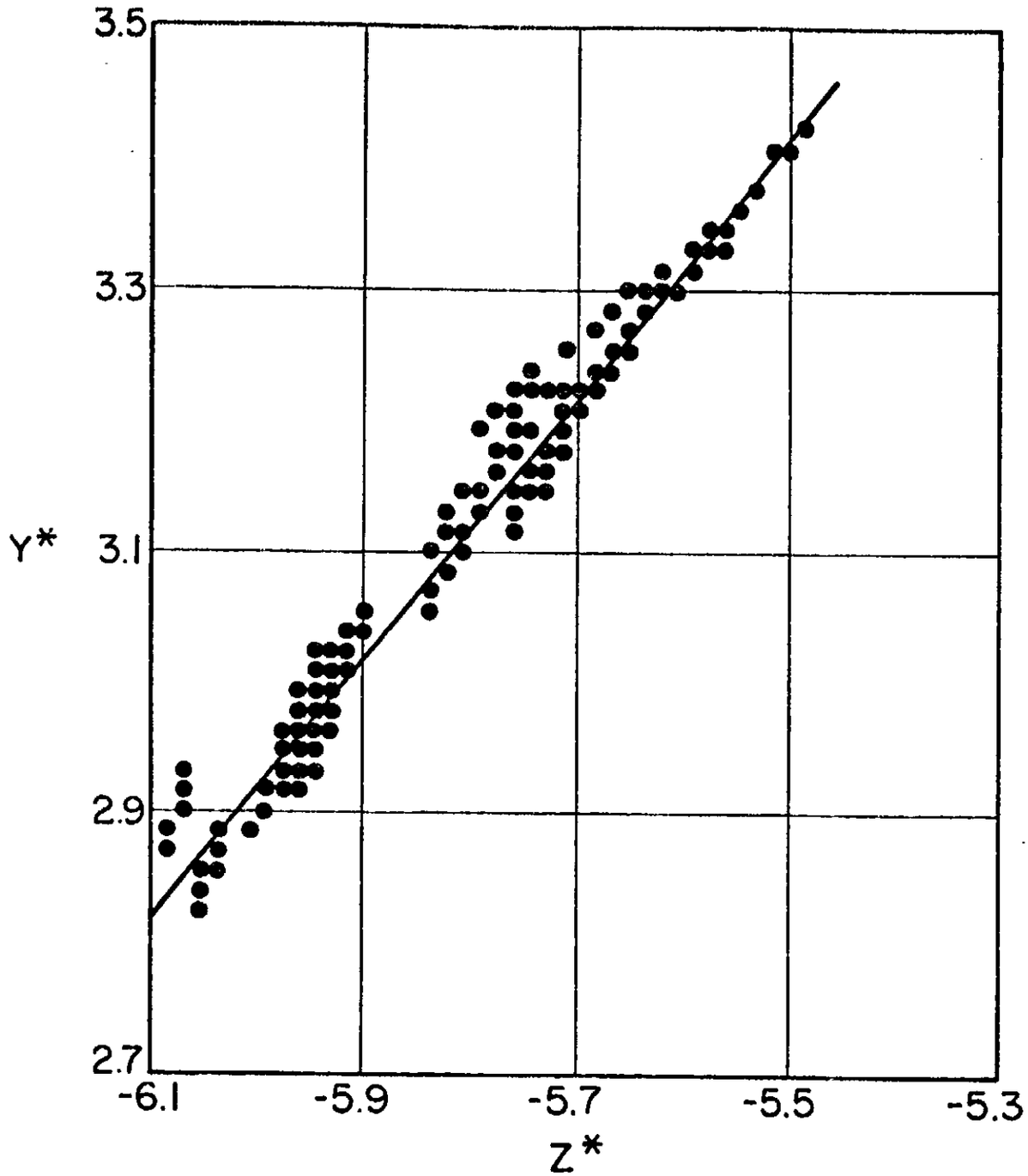

Figure 8. Data Collapse About Correlation (8.15)

8.5 General Remarks

a. The increase of D discussed in section 8.3, resulted in a better fit. This can be explained as follows : In the process of deriving Equation (8.4), the non-dimensional effective center of the probe, k_{eff} , is assumed to be unity. Patel [16] and Prozorov [22] and others, e.g. Chue [17], have found that $0.55<y_{eff}/D<0.65$. Thus, writing Equation (8.4) in the form

$$\frac{\Delta P}{\tau_w} g\left[\frac{u^* D_{eq}}{2 \nu}\right], \quad D_{eq} \approx 1.3D$$

is equivalent to assuming that the average value of $y_{eff} \approx 1.3\ D/2 \approx 0.65\ D$, or equivalently $k_{eff} \approx 1.3$.

The better fit is an indication of the strong effect of the probe geometry expressed by R_D. One can also conclude that k_{eff} is a function of R_D. This conclusion was postulated before by Preston [21]. Patel [16] and Prozorov [22] showed that k_{eff} is a function of $u_{pt} D/\nu$.

b. Although the assumption that k_{eff} is a constant works well, k_{eff} is not a constant in fact. This can be seen in Figure 6. It increases slowly with x. It can be shown that a constant k_{eff} requires that the coefficient of x^* in the correlation be 0.5. The higher coefficient in Equation (8.10) confirms that k_{eff} is not a constant. Assuming a Blasius type profile, it is shown in Appendix D that $k_{eff} \alpha (x/D)^{.337}/(Re_x)^{.355}$.

c. The correlation (8.15) is true for body geometries other than the cone since it is based on local variables. It

accounts for heat transfer conditions since it includes the temperature ratio T^*/T_e. It is also thought to be valid for pressure gradients since it is based on conditions near the wall. Thus, it is considered to be a general equation for estimation of skin-friction coefficients in subsonic, laminar boundary layers.

d. In an attempt to improve the curve-fit, we tried various calibration models. Among them were the following results :

$$y^* = 0.102\, x^* - 0.232 \log_{10} M_\infty + 0.815 \log_{10} Re_{ft} - 0.867 \log_{10} \frac{\theta}{D} - 3.458 \qquad (8.18a)$$

with an rms error of 0.27%,

$$y^* = 0.011\, x^* - 0.582 \log_{10} (1+M_\infty^2) + 0.481 \log_{10} Re_x - 1.972 \log_{10} \frac{\theta}{D} - 1.554 \qquad (8.18b)$$

with an rms error of 0.06%, and

$$\log_{10} \frac{1}{c_f} = 0.002 \log_{10} [(P_{Pt} - P_\infty/q_\infty] + 0.024 \log_{10} (1+M_\infty 2) + 0.501 \log_{10} (Re_{ft}\, D\, \frac{x}{L}) + 1.688 \qquad (8.18c)$$

with an rms error of 0.02%. Though the accuracy of the fit became better and better, the dependence on x^* and the Preston-tube measurements became less and less. This means that STAN5 calculations were correlated in these calibration models rather than the experimental data.

The use of freestream parameters (M_∞, Re_{ft}) in correlations (8.18a,b,c) limits their use to the 10-degree cone measurements, i.e., the coefficients of M_∞ and Re_{ft} in these correlations are not universal. To correct for that, the local Mach number M_e and Re_x should be used.

e. The calibration models used by Bradshaw and Unsworth, Allen, Fenter and Stallmach, and Patel which were reported by Allen in his survey report [20] were all tried for the present laminar data. It was found that none of them was competitive with our correlation in terms of the rms error in skin-friction coefficient. Allen's 2nd-degree model fitted the laminar data with an rms error in C_f of 8.64.

f. Bradshaw and Unsworth [23] have criticized Allen's use of the reference temperature to evaluate density and viscosity in the classical law-of-the-wall. Rather than replace the conventional evaluation of properties at the wall, we have followed the procedure by Tetervin [18] and others to obtain a compressible equation for C_f by simply multiplying an incompressible equation for C_f by the ratio of T'/T_e raised to some exponent. Here we have determined the exponent via a curve fit of the data. Thus, we are partially accounting for Bradshaw and Unsworth's objection. However, their second objection still applies to our analysis in that the reference temperature method is based on zero-pressure-gradient flows and has an unknown range of validity for flows with pressure gradients.

8.6 Prozorov Correlation

Assuming a relatively small height of the Preston-tube, Prozorov [22] expanded the velocity u about the wall using Maclaurin's series and reached the following simple correlation for incompressible laminar boundary layers.

$$C_f = \frac{1}{q_e}\left(\frac{\mu u_{pt}}{y_{eff}} - \frac{1}{2} y_{eff} \frac{dP}{dx}\right) \qquad (8.19)$$

We analytically verified Equation (8.19) for round and rectangle openings of the probe (for which y_{eff} can be theoretically calculated).

Correlation (8.19) has the advantage that it can be used for high pressure gradients*, and the disadvantage that y_{eff} must be known a priori.
It is also limited to incompressible flows.

It is worth mentioning that Prozorov's paper is the only study found in the literature that discusses correlating Preston-tube data with theoretical laminar shear stress.

---

*All the cases investigated in this study had small favorable dP/dx.

CHAPTER IX

CONCLUSIONS

1. The Wu and Lock computer program is an accurate and reliable way of calculating the inviscid flow field about a sharp cone at transonic speeds.

With the added subroutines, the program is now capable of calculating the inviscid pressure and velocity distribution along a conical ray, corresponding to the Preston tube survey, for arbitrary combinations of pitch and yaw angles. It also calculates compressible initial profiles based on similarity theory and the supersonic laminar cone rule; this information is used to start the boundary layer computations.

2. The STAN5 computer code does not work satisfactorily when the flow angles are significant. It was found that its calculations were insensitive to changes in the flow angles when other parameters were kept the same. This limits its utility.

3. It is possible to correlate skin friction and experimental Preston-tube pressure measurements in the simple form (8.17).

4. The non-dimensional effective center of the Preston tube, k_{eff}, is not a constant value but rather increases with x and decreases with Re_x.

CHAPTER X

SUPPLEMENTARY OBSERVATIONS

1. A 3-dimensional boundary-layer computer code is needed to continue investigation of the role of pitch and yaw angles on the correlation of Preston-tube data and skin friction.

2. The laminar correlation needs to be verified in supersonic flows and also for free-flight conditions for which the wall temperature seldom equals the adiabatic wall temperature.

3. By using the measured Preston-tube pressures at the end of transition, the correlation of Allen [20] can be used to initiate computation of the fully-developed turbulent boundary layers on the cone. This avoids tackling the development of a skin-friction correlation for the boundary-layer transition region until the laminar and turbulent correlations are established.

4. The laminar correlation may be connected with Allen's and/or Bradshaw and Unsworth's [20] correlations for turbulent boundary layers in order to model boundary-layer transition.

5. In order to verify and make use of Prozorov's [22] findings, a method is required that relates the Preston-tube pressure to the geometry of the probe. One way of doing this

is by curve-fitting the computed values of k_{eff} (obtained from plots similar to Figure 6) with x and Re_x.

BIBLIOGRAPHY

(1) NASA/Ames 11-Ft Transonic Wind Tunnel Measurements. NASA/Ames Research Center, Moffet Field, California. March 1975.

(2) Crawford, M. E. and W. M. Kays, "STAN5 - A Program For Numerical Computation of Two-Dimensional Internal/External Boundary Layer Flows". Report No. HMT-23, Department of Mechanical Engineering, Stanford University. December 1975.

(3) Patankar, S. V. and D. B. Spalding, Heat and Mass Transfer in Boundary Layers. 2nd Edition. Intertext Books, London. 1970.

(4) Wu, J. and R. C. Lock, "A Theory for Subsonic and Transonic Flow Over a Cone - With and Without Small Yaw Angle". Technical Report RD-74-2, U. S. Army Missile Command. December 1973.

(5) Huprikar, A. G., "Evaluation Method for Transonic Cone Boundary Layer Transition Data by Means of Computer Simulation". Oklahoma State University. December 1978.

(6) Davis, J. W., "Optimization of Wave Cancellation in Variable Porosity Transonic Wind Tunnel Flows". George C. Marshall Space Flight Center, Alaska. November 1973.

(7) Goin, K. L., "The History, Evolution and Use of Wind Tunnels". AIAA Student Journal. February 1971.

(8) Reed, T. D., T. C. Pope and J. M. Cooksey, "Calibration of Transonic and Supersonic Wind Tunnels". NASA CR 2920. November 1977.

(9) Dougherty, N. S., Jr., Private Communication. November 1979.

(10) Chandler, J. P. and L. W. Jackson, "Subroutine MARQ, Version 2.6, A.N.S.I. Standard FORTRAN". WATFIV Library, University Computer Center, Oklahoma State University. February 1979.

(11) Dunn, M., R. Jones and M. Zissen, "Computer Program for Calculation of Effective Angle of Attack and Location of Windward Element". Report TIAD 661. Interdepartmental Communication. Lockheed Aircraft Corporation. 14 November 1963.

(12) Equations, Tables and Charts for Compressible Flow. Ames Research Staff. NACA Report 1135. Ames Aeronautical Laboratory, Moffet Field, California.

(13) White, F. M., Viscous Fluid Flow, McGraw-Hill Book Co. New York. 1974.

(14) Whitfield, J. D. and N. S. Dougherty, Jr., "A Survey of Transition Research at AEDC". AGARD Conference Proceeding No. 224.

(15) Dougherty, N. S., Jr. and D. F. Fisher, "Boundary Layer Transition on a 10-Degree Cone : Wind Tunnel/Flight Data Correlation". AIAA 18th Aerospace Sciences Meeting. Pasadena, California. January 14-16, 1980.

(16) Patel, V. C., "Calibration of the Preston Tube and Limitations on its Use in Pressure Gradients". J. Fluid Mechanics, Vol. 23, pp. 185-208. 1965.

(17) Chue, S. H., "Pressure Probes for Fluid Measurement". Prog. Aerospace Sci., Vol. 16, No. 2, pp. 147-221. 1975.

(18) Tetervin, N., "A Transformation between Axisymmetric and two-Dimensional Turbulent Boundary Layers". AIAA Journal, Vol. 8, No. 5, pp. 985-987. May 1970.

(19) Schlichting, H., Boundary Layer Theory, McGraw-Hill Book Co. 1968.

(20) Allen, J. M., "Reevaluation of Compressible-Flow Preston Tube Calibrations". NASA TM X-3488. February 1977.

(21) Preston, J. H., "Determining Skin Friction with Pitot Tubes". J. Royal Aeronautical Society, 54, 518. 1954.

(22) Prozorov, A. G., "Determinations of the Skin Friction in the Boundary Layer with a Small Pitot Probe". Fluid Mechanics Soviet Research, Vol. 5, No. 6. November-December 1976.

(23) Bradshaw, P. and K. Unsworth, "Comment on Evaluation of Preston Tube Calibration Equations in Supersonic Flow". AIAA Journal, Vol. 12, No. 9, pp. 1293-1296. September 1974.

APPENDIX A

AZIMUTH ANGLE CALCULATION

In this appendix are presented the equations developed by Dunn et al [11] to locate the windward element. Figure 9 is a schematic of a typical vehicle at angle of attack which defines the parameters used in this appendix. As illustrated, the angles of pitch and yaw are measured with respect to the freestream velocity vector. It should be noted that the relationship utilized to determine the location of the windward element is sensitive to calculation accuracy. For this reason, double precision is used in the computer subprogram ANGLES. The pitch and yaw angles are restricted to magnitudes less than 90 degrees.

The first step is to evaluate the angle between the vehicle axis and the resolved yaw vector. This angle will be denoted by ϕ.

$$\sin(\phi) = c/f$$

$$\tan(\phi) = c/d$$

$$\sin(\alpha) = c/e$$

$$\tan(\alpha) = c/a$$

$$\sin(\alpha)/\sin(\phi) = (c/e)/(c/f) = f/e$$

$$\tan(\alpha)/\tan(\phi) = (c/a)/(c/d) = d/a$$

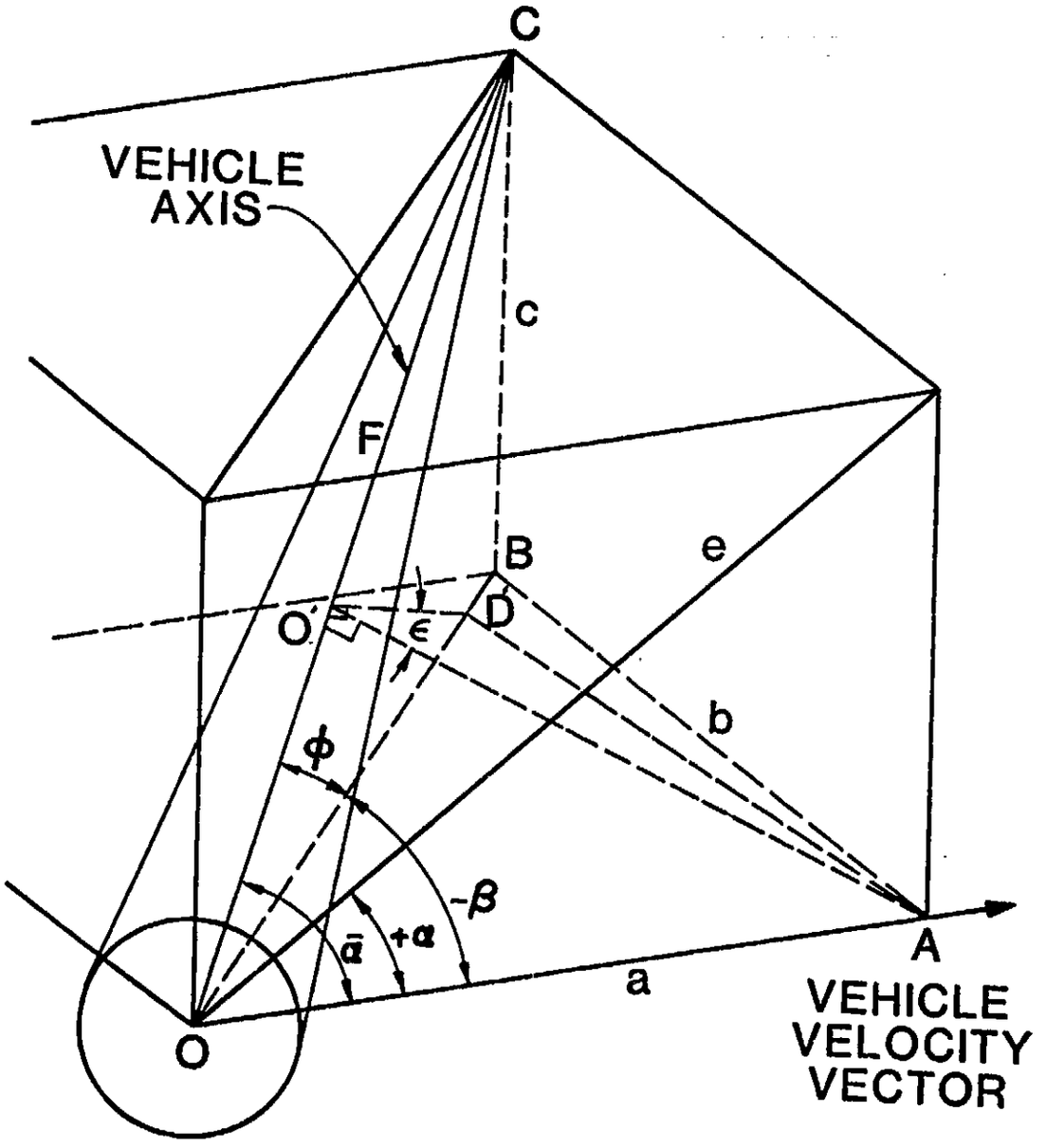

Figure 9. Schematic of Flow Angles

$$\cos(\beta) = a/d$$

Thus $\tan(\phi) = (a/d)\tan(\alpha) = \cos(\beta)\tan(\alpha)$

$$\tan(\phi) = \cos(\beta)\tan(\alpha) \qquad (A.1)$$

Now the angle $\bar{\alpha}$ can be calculated as follows :

$$d/f = \cos(\phi),\ \cos(\bar{\alpha}) = a/f = (a/d)(d/f)$$

$$\therefore \cos(\bar{\alpha}) = \cos(\beta)\cos(\phi),\ 0<\bar{\alpha}<90 \qquad (A.2)$$

Equation (A.2) determines the angle $\bar{\alpha}$ which is denoted as the effective angle of attack.

At this point, we want to find the angle that the windward vector makes with the vehicle axis. The following results can be obtained from Figure 9.

$$\cos(\epsilon) = (O'D')/(O'A)$$

$$O'A = a\sin(\bar{\alpha})$$

$$O'O = a\cos(\bar{\alpha})$$

$$\tan(\phi) = (O'D')/(O'O)$$

$$\cos(\epsilon) = (O'D')/a\sin(\bar{\alpha}) = (O'O)\tan(\phi)/a\sin(\bar{\alpha})$$

$$\cos(\epsilon) = a\cos(\bar{\alpha})\tan(\phi)/a\sin(\bar{\alpha})$$

$$\therefore \cos(\epsilon) = \cot(\bar{\alpha})\tan(\phi) \qquad (A.3)$$

an alternate expression for calculating ϵ can be formed by substituting Equation (A.1) for $\tan(\phi)$

$$\cos(\epsilon) = \cot(\bar{\alpha})\cos(\beta)\tan(\alpha)$$

APPENDIX B

CALCULATION OF FREESTREAM PROPERTIES

Values of M_∞ , q_∞ and Re_{ft} are specified for a given wind tunnel setting. From these values, all properties of the freestream can be calculated as follows :

1. Obtain the freestream total pressure $P_{t,\infty}$ as follows :

$$q_\infty = \frac{1}{2} \rho_\infty U_\infty^2 = \frac{1}{2} \rho_\infty M_\infty^2 (\gamma P_\infty/\rho_\infty) = \gamma M_\infty^2 P_\infty/2 \qquad (B.1)$$

$$P_{t,\infty} = \frac{P_{t,\infty}}{P_\infty} \cdot \frac{P_\infty}{q_\infty} \cdot q_\infty = 2 q_\infty \left(1 + \frac{\gamma-1}{2} M_\infty^2\right)^{\gamma/(\gamma-1)} / \gamma M_\infty^2 \qquad (B.2)$$

Note that the total pressure and temperature are constant for isentropic, subsonic flow.

2. Obtain the freestream static temperature as follows :

$$\frac{M_\infty Re_{ft}}{q_\infty} = \frac{U_\infty}{\sqrt{\gamma R T_\infty}} \frac{\rho_\infty U_\infty}{\mu_\infty} \cdot \frac{2}{\rho_\infty U_\infty^2} = \frac{2}{\mu_\infty \sqrt{\gamma R T_\infty}}$$

$$= \frac{2 (T_\infty + 198.6)}{2.27 \times 10^{-8} T_\infty^{1.5} \sqrt{\gamma R T_\infty}}$$

$$\therefore \left(\frac{M_\infty Re_{ft}}{q_\infty} \cdot \frac{2.27 \times 10^{-8} \gamma R}{2}\right) T_\infty^2 - T_\infty - 198.6 = 0 \qquad (B.3)$$

Where Sutherland's relation is used for μ_∞.

3. Using Equations (B.1) and (B.3), ρ_∞ can be obtained from the the perfect gas relation :

$$\rho_\infty = P_\infty / R T_\infty \qquad (B.4)$$

4. Also the total temperature can be found using the isentropic relation :

$$T_t = T_\infty \left(1 + \frac{\gamma-1}{2} M_\infty^2\right) \qquad (B.5)$$

This procedure is automated in subroutine DIST of the exterded Wu and Lock program described in Chapter V. The listing of the routine can be found in Appendix F.

APPENDIX C

CALCULATION OF INITIAL PROFILES

Since STAN5 is a forward-marching, finite-difference program, starting profiles of velocity and total enthalpy are required to calculate subsequent velocity and total enthalpy profiles along the cone. Care should be taken, therefore, in calculating these initial profiles. However, the effect of the starting profile on the calculations becomes small after a certain developmental distance, as shown in Figure 1.

The edge velocity distribution can be expressed [13] as follows

$$U_e = c\, x^n \qquad \text{(C.1)}$$

Where c and n are constants. Fitting Equation (C.1) to typical edge velocities near the tip of the cone, as obtained from the extended Wu and Lock program[4], results in n_c = 0.0047.

The pressure gradient parameter for a conical flow, β, is related to the inviscid velocity distribution [13] by

$$\beta_c = \frac{2n}{3+n} = 0.003128.$$

This in turn corresponds to a wedge flow with

$$n_w = n_c/3 = 0.00157.$$

---

[4]Case analyzed here was Case 40.547.

Examination of Figure 4-11 of White [13] indicates that the solution for $f(\eta)$ corresponding to $\beta = 0$ is expected to be good. Therefore, the tabulated solution for Blasius flow may be used to specify the initial profiles. The normal distance y_c can be calculated now from

$$y_c = y_B/\sqrt{3}$$

$$\therefore \quad y_c = \eta_B \Big/ \left[\frac{3\ U_e}{2\ \nu'\ x}\right]^{.5} \qquad \text{(C.2)}$$

Where ν' is the kinematic viscosity evaluated at the reference temperature T' as will be shown now. One can obtain Equation (C.2) using Mangler transformation.

An expression for the reference temperature across the boundary layer is given by Eckert's formula [13] :

$$T' = T(0.5 + 0.039\ M^2 + 0.5\ T_w/T) \qquad \text{(C.3)}$$

Where
$$T = T_t/(1 + \frac{\gamma-1}{2} M^2) \qquad \text{(C.4)}$$

and
$$T_w = T_{aw} = T(1 + r\ \frac{\gamma-1}{2} M^2) \qquad \text{(C.5)}$$

Where $r = (Pr)^{1/2}$ for laminar boundary layer, and

$= (Pr)^{1/3}$ for turbulent boundary layer.

The values of local Mach numbers M_e and the total temperature T_t are calculated by the extended Wu and Lock program. Prandtl number is taken to be 0.72 for air.

Now μ' can be calculated using Sutherland's relation

$$\mu' = 2.27 \times 10^{-8}\ \frac{(T')^{1.5}}{T' + 198.6} \qquad \text{(C.6)}$$

To obtain ν', ρ' is calculated using the perfect gas relation

$$\rho' = P_w/R\ T' \qquad \text{(C.7)}$$

Where the static pressure P_w is calculated in the main Wu and Lock program.

Therefore, from (C.6) and (C.7), ν' can be calculated,

$$\nu' = \mu'/\rho' \tag{C.8}$$

Substitution in (C.2), yields a table of y_c vs. η_B. From the Blasius solution for $t' = u/U_e$, we can obtain a table of u vs. η_B. Thus the initial velocity profile is specified.

The total enthalpy is defined as

$$h_t = h + \frac{u^2}{2 g_c J}$$

$$= c_p T + \frac{u^2}{2 g_c J} \qquad \text{for } c_p = \text{constant} \tag{C.9}$$

The distribution of T through the boundary layer may be approximately expressed [13] as

$$T \simeq T_w + (T_{aw} - T_w) \frac{u}{U_e} - \frac{r u^2}{2 c_p g_c J}$$

Substitution into (C.9) gives

$$h_t = c_p \left[T_w - (T_{aw} - T_w) \frac{u}{U_e}\right] + \frac{(1 - r) u^2}{2 g_c J}$$

With the assumption $T_w = T_{aw}$, this equation reduces to

$$h_t = c_p T_w + \frac{(1 - r) u^2}{2 g_c J} \tag{C.10}$$

T_w was calculated via the Wu and Lock program, and the initial stagnation profile was defined by Equation (C.10).

APPENDIX D

FUNCTIONAL DEPENDENCE OF THE EFFECTIVE CENTER OF THE PROBE

For simplicity, we will derive an expression for k_{eff} for incompressible flow over a flat plate. The correlation (8.14) reduces in this case to

$$C_f \sim C_p^{0.655} R_D^{0.69} \qquad \text{(D.1)}$$

where $C_f = \tau_w/(0.5 \rho U^2)$,

$C_p = \Delta P /(0.5 \rho U^2)$,

$R_D = U D/\nu = (U x/\nu) D/x = Re_x D/x$. Since $\Delta P = \frac{1}{2} \rho u_{Pt}^2$ C_p can be written in the form

$$C_p = (u_{Pt}/U)^2 = (f')^2 \text{ at } \eta_{eff},$$

where f' = 1st derivative of the Blasius function w.r.t. η, and

$$\eta_{eff} = y_{eff} \sqrt{U/2 \nu x} \sim k_{eff} D \sqrt{Re_x}/x.$$

Since the height of the probe is very small (0.0097"), all the laminar boundary-layer data was obtained within the lower 40% of the layer thickness. In this region $f' \sim \eta$ is valid.

Therefore, C_p can be expressed as

$$C_p \sim \eta_{eff}^2 \sim k_{eff}^2 D^2 Re_x/x^2. \qquad \text{(D.2)}$$

Substituting relation (D.2) into (D.1) gives

$$C_f \sim k_{eff}^{1.31} Re_x^{-0.035} \left(\frac{x}{D}\right)^{-0.441} \qquad \text{(D.3)}$$

The well-known relation for C_f in this case is

$$C_f \sim Re_x^{-0.5} \tag{D.4}$$

Comparing (D.3) and (D.4), the following equation is obtained for k_{eff}.

$$k_{eff} \sim Re_x^{-0.355} \left(\frac{x}{D}\right)^{0.337} \tag{D.5a}$$

Or alternatively, $k_{eff} \sim Re_x^{-0.018} R_D^{-0.337}$ (D.5b)

Again, relations (D.5a,b) are only valid for incompressible flow over a flat plate and are presented here only to demonstrate that y_{eff} is not a constant.

APPENDIX E

RAW DATA USED FOR SKIN-FRICTION CORRELATION

POINT NO.	MINF	REFT	QINF	X	DELTAP	PINF	UE	RHOW	RHOE	NUW	NUE	THETA	CF
1	0.60	0.50E 07	586.0	4.5	323.6	2325.0	636.3	0.084127	0.088915	0.14414E-03	0.13046E-03	0.0001065	0.000864
2	0.60	0.50E 07	586.0	5.0	306.5	2325.0	636.6	0.084103	0.088899	0.14419E-03	0.13047E-03	0.0001123	0.000820
3	0.60	0.50E 07	586.0	5.5	293.7	2325.0	636.9	0.084084	0.088883	0.14422E-03	0.13049E-03	0.0001174	0.000780
4	0.60	0.50E 07	586.0	6.0	279.4	2325.0	637.2	0.084058	0.088869	0.14427E-03	0.13050E-03	0.0001228	0.000748
5	0.60	0.50E 07	586.0	6.5	268.0	2325.0	637.5	0.084054	0.088855	0.14426E-03	0.13051E-03	0.0001278	0.000718
6	0.60	0.50E 07	586.0	7.0	255.2	2325.0	637.8	0.084036	0.088841	0.14429E-03	0.13053E-03	0.0001324	0.000692
7	0.60	0.50E 07	586.0	7.5	246.6	2325.0	638.1	0.084021	0.088829	0.14431E-03	0.13054E-03	0.0001370	0.000668
8	0.60	0.40E 07	477.0	4.0	286.5	1893.0	640.2	0.067588	0.071424	0.18135E-03	0.16420E-03	0.0001123	0.001026
9	0.60	0.40E 07	477.0	4.5	270.9	1893.0	640.5	0.067564	0.071410	0.18143E-03	0.16422E-03	0.0001191	0.000966
10	0.60	0.40E 07	477.0	5.0	252.3	1893.0	640.9	0.067546	0.071397	0.18148E-03	0.16424E-03	0.0001253	0.000918
11	0.60	0.40E 07	477.0	5.5	238.1	1893.0	641.3	0.067531	0.071384	0.18152E-03	0.16426E-03	0.0001314	0.000874
12	0.60	0.40E 07	477.0	6.0	228.1	1893.0	641.6	0.067510	0.071373	0.18159E-03	0.16428E-03	0.0001370	0.000838
13	0.60	0.40E 07	477.0	6.5	221.0	1893.0	641.9	0.067508	0.071361	0.18157E-03	0.16430E-03	0.0001427	0.000804
14	0.60	0.40E 07	477.0	7.0	215.3	1893.0	642.1	0.067495	0.071350	0.18159E-03	0.16431E-03	0.0001483	0.000772
15	0.60	0.40E 07	477.0	7.5	209.6	1893.0	642.4	0.067483	0.071340	0.18163E-03	0.16433E-03	0.0001533	0.000746
16	0.60	0.40E 07	477.0	8.0	203.9	1893.0	642.7	0.067468	0.071330	0.18167E-03	0.16435E-03	0.0001584	0.000722
17	0.60	0.30E 07	357.0	6.5	139.7	1417.0	641.5	0.050595	0.053491	0.24196E-03	0.21889E-03	0.0001652	0.000926
18	0.60	0.30E 07	357.0	7.0	136.5	1417.0	641.8	0.050584	0.053483	0.24202E-03	0.21892E-03	0.0001713	0.000894
19	0.60	0.30E 07	357.0	7.5	132.6	1417.0	642.1	0.050573	0.053475	0.24207E-03	0.21894E-03	0.0001773	0.000862
20	0.60	0.30E 07	357.0	8.0	129.7	1417.0	642.3	0.050566	0.053469	0.24210E-03	0.21896E-03	0.0001825	0.000838
21	0.60	0.30E 07	357.0	8.5	126.5	1417.0	642.6	0.050559	0.053461	0.24212E-03	0.21898E-03	0.0001885	0.000810
22	0.60	0.30E 07	357.0	9.0	124.0	1417.0	642.8	0.050552	0.053454	0.24214E-03	0.21900E-03	0.0001936	0.000788
23	0.60	0.30E 07	357.0	9.5	121.2	1417.0	643.0	0.050542	0.053447	0.24219E-03	0.21902E-03	0.0001989	0.000768
24	0.60	0.30E 07	357.0	10.0	118.3	1417.0	643.3	0.050539	0.053440	0.24219E-03	0.21904E-03	0.0002041	0.000748
25	0.60	0.30E 07	357.0	10.5	116.9	1417.0	643.5	0.050526	0.053433	0.24226E-03	0.21906E-03	0.0002089	0.000732
26	0.60	0.30E 07	357.0	11.0	112.6	1417.0	643.8	0.050526	0.053427	0.24223E-03	0.21907E-03	0.0002137	0.000714
27	0.60	0.40E 07	404.0	5.0	215.3	2309.0	537.8	0.082484	0.085747	0.14800E-03	0.13802E-03	0.0001259	0.000916
28	0.60	0.40E 07	404.0	5.5	209.6	2309.0	538.1	0.082471	0.085737	0.14803E-03	0.13803E-03	0.0001318	0.000876
29	0.60	0.40E 07	404.0	6.0	201.0	2309.0	538.3	0.082461	0.085727	0.14804E-03	0.13804E-03	0.0001377	0.000836
30	0.60	0.40E 07	404.0	6.5	193.9	2309.0	538.6	0.082458	0.085718	0.14803E-03	0.13805E-03	0.0001433	0.000804
31	0.60	0.40E 07	404.0	7.0	188.2	2309.0	538.8	0.082451	0.085709	0.14804E-03	0.13806E-03	0.0001483	0.000776
32	0.60	0.40E 07	404.0	7.5	182.5	2309.0	539.0	0.082436	0.085701	0.14807E-03	0.13807E-03	0.0001536	0.000750
33	0.60	0.40E 07	404.0	8.0	178.2	2309.0	539.3	0.082428	0.085692	0.14808E-03	0.13808E-03	0.0001586	0.000726
34	0.60	0.40E 07	404.0	8.5	173.5	2309.0	539.5	0.082418	0.085684	0.14810E-03	0.13809E-03	0.0001634	0.000704
35	0.60	0.40E 07	404.0	9.0	171.1	2309.0	539.7	0.082409	0.085677	0.14811E-03	0.13810E-03	0.0001672	0.000684
41	0.60	0.30E 07	302.0	6.5	122.6	1726.0	538.0	0.061786	0.064239	0.19717E-03	0.18383E-03	0.0001654	0.000930
42	0.60	0.30E 07	302.0	7.0	118.3	1726.0	538.2	0.061779	0.064232	0.19719E-03	0.18384E-03	0.0001714	0.000898

POINT NO.	MINF	REFT	GINF	X	DELTAP	PINF	UE	RHOW	RHOE	NUW	NUE	THETA	CF
43	0.50	0.30E 07	302.0	7.5	116.9	1726.0	536.4	0.061765	0.064226	0.19722E-03	0.18385E-03	0.0001773	0.000866
44	0.50	0.30E 07	302.0	8.0	115.5	1726.0	538.7	0.061767	0.064219	0.19721E-03	0.18386E-03	0.0001833	0.000838
45	0.50	0.30E 07	302.0	8.5	112.6	1726.0	538.9	0.061763	0.064214	0.19722E-03	0.18388E-03	0.0001888	0.000814
46	0.50	0.30E 07	302.0	9.0	111.2	1726.0	539.1	0.061753	0.064207	0.19725E-03	0.18389E-03	0.0001944	0.000790
47	0.50	0.30E 07	302.0	9.5	108.3	1726.0	539.3	0.061748	0.064201	0.19726E-03	0.18390E-03	0.0001996	0.000768
48	0.50	0.30E 07	302.0	10.0	105.5	1726.0	539.5	0.061742	0.064196	0.19727E-03	0.18391E-03	0.0002048	0.000748
49	0.50	0.30E 07	302.0	10.5	102.6	1726.0	539.7	0.061739	0.064190	0.19728E-03	0.18392E-03	0.0002096	0.000732
50	0.50	0.30E 07	302.0	11.0	101.2	1726.0	539.9	0.061735	0.064185	0.19728E-03	0.18392E-03	0.0002144	0.000714
51	0.50	0.30E 07	302.0	11.5	98.4	1726.0	540.1	0.061728	0.064179	0.19730E-03	0.18394E-03	0.0002191	0.000700
52	0.70	0.40E 07	548.0	4.5	306.5	1598.0	742.4	0.056807	0.061196	0.21734E-03	0.19005E-03	0.0001190	0.000964
53	0.70	0.40E 07	548.0	5.0	285.1	1598.0	742.8	0.056785	0.061181	0.21743E-03	0.19012E-03	0.0001252	0.000914
54	0.70	0.40E 07	548.0	5.5	266.6	1598.0	743.1	0.056767	0.061168	0.21750E-03	0.19015E-03	0.0001309	0.000874
55	0.70	0.40E 07	548.0	6.0	256.6	1598.0	743.5	0.056744	0.061153	0.21760E-03	0.19018E-03	0.0001371	0.000834
56	0.70	0.40E 07	548.0	6.5	246.6	1598.0	743.9	0.056738	0.061140	0.21759E-03	0.19020E-03	0.0001428	0.000800
57	0.70	0.40E 07	548.0	7.0	238.1	1598.0	744.2	0.056723	0.061128	0.21765E-03	0.19023E-03	0.0001479	0.000772
58	0.70	0.40E 07	548.0	7.5	230.9	1598.0	744.5	0.056712	0.061117	0.21768E-03	0.19025E-03	0.0001529	0.000746
59	0.70	0.40E 07	548.0	8.0	223.8	1598.0	744.8	0.056692	0.061105	0.21777E-03	0.19028E-03	0.0001580	0.000722
60	0.70	0.50E 07	680.0	4.5	365.0	1983.0	740.2	0.070907	0.076384	0.17328E-03	0.15157E-03	0.0001061	0.000862
61	0.70	0.50E 07	680.0	5.0	343.6	1983.0	740.6	0.070882	0.076366	0.17335E-03	0.15160E-03	0.0001119	0.000816
62	0.70	0.50E 07	680.0	5.5	329.3	1983.0	741.0	0.070854	0.076349	0.17343E-03	0.15162E-03	0.0001173	0.000780
63	0.70	0.50E 07	680.0	6.0	313.6	1983.0	741.3	0.070827	0.076332	0.17350E-03	0.15164E-03	0.0001224	0.000746
64	0.70	0.50E 07	680.0	6.5	296.5	1983.0	741.7	0.070818	0.076316	0.17350E-03	0.15167E-03	0.0001273	0.000716
65	0.70	0.30E 07	408.0	5.5	161.1	1190.0	741.1	0.042554	0.045805	0.28912E-03	0.25272E-03	0.0001518	0.001008
66	0.70	0.30E 07	408.0	6.0	155.4	1190.0	741.5	0.042489	0.045795	0.28924E-03	0.25276E-03	0.0001582	0.000966
67	0.70	0.30E 07	408.0	6.5	151.1	1190.0	741.8	0.042480	0.045785	0.28928E-03	0.25279E-03	0.0001650	0.000924
68	0.70	0.30E 07	408.0	7.0	146.8	1190.0	742.1	0.042470	0.045776	0.28933E-03	0.25283E-03	0.0001710	0.000892
69	0.70	0.30E 07	408.0	7.5	142.6	1190.0	742.4	0.042457	0.045767	0.28943E-03	0.25286E-03	0.0001768	0.000860
70	0.70	0.30E 07	408.0	8.0	138.3	1190.0	742.7	0.042446	0.045759	0.28951E-03	0.25289E-03	0.0001823	0.000836
71	0.70	0.30E 07	408.0	8.5	135.4	1190.0	743.0	0.042437	0.045751	0.28957E-03	0.25292E-03	0.0001879	0.000810
72	0.70	0.30E 07	408.0	9.0	132.6	1190.0	743.3	0.042429	0.045742	0.28959E-03	0.25295E-03	0.0001935	0.000786
73	0.70	0.30E 07	408.0	9.5	128.3	1190.0	743.6	0.042423	0.045735	0.28962E-03	0.25298E-03	0.0001988	0.000766
74	0.70	0.30E 07	408.0	10.0	125.5	1190.0	743.8	0.042411	0.045728	0.28971E-03	0.25301E-03	0.0002036	0.000748
75	0.70	0.30E 07	408.0	10.5	122.6	1190.0	744.1	0.042402	0.045720	0.28977E-03	0.25304E-03	0.0002086	0.000730
76	0.40	0.40E 07	403.0	6.5	162.5	3598.0	470.4	0.109310	0.112030	0.12600E-03	0.12066E-03	0.0001430	0.000806
77	0.40	0.40E 07	403.0	7.0	156.8	3598.0	470.6	0.109300	0.112020	0.12601E-03	0.12067E-03	0.0001486	0.000776
78	0.40	0.40E 07	403.0	7.5	152.5	3598.0	470.8	0.109290	0.112010	0.12602E-03	0.12067E-03	0.0001536	0.000750
79	0.40	0.40E 07	403.0	8.0	149.7	3598.0	471.0	0.109280	0.112010	0.12603E-03	0.12068E-03	0.0001586	0.000726

POINT NO.	MINF	REFT	CINF	X	DELTAP	PINF	UE	RHOW	RHOE	NUW	NUE	THETA	CF
80	0.40	0.40E 07	403.0	8.5	145.4	3558.0	471.2	0.109280	0.112000	0.12602E-03	0.12068E-03	0.0001634	0.000704
81	0.40	0.30E 07	246.0	6.5	102.6	2196.0	433.6	0.078472	0.080454	0.15514E-03	0.14833E-03	0.0001657	0.000930
82	0.40	0.30E 07	246.0	7.0	101.2	2196.0	433.8	0.078467	0.080449	0.15515E-03	0.14833E-03	0.0001716	0.000898
83	0.40	0.30E 07	246.0	7.5	98.4	2196.0	434.0	0.078463	0.080444	0.15515E-03	0.14834E-03	0.0001775	0.000868
84	0.40	0.30E 07	246.0	8.0	96.9	2196.0	434.2	0.078455	0.080438	0.15517E-03	0.14835E-03	0.0001834	0.000838
85	0.40	0.30E 07	246.0	8.5	95.5	2196.0	434.3	0.078460	0.080434	0.15514E-03	0.14835E-03	0.0001886	0.000816
86	0.40	0.30E 07	246.0	9.0	94.1	2196.0	434.5	0.078451	0.080429	0.15517E-03	0.14836E-03	0.0001945	0.000790
87	0.40	0.30E 07	246.0	9.5	92.7	2196.0	434.7	0.078444	0.080424	0.15518E-03	0.14836E-03	0.0001996	0.000770
88	0.40	0.30E 07	246.0	10.0	85.8	2196.0	434.9	0.078437	0.080415	0.15519E-03	0.14837E-03	0.0002048	0.000750
89	0.40	0.30E 07	246.0	10.5	88.4	2196.0	435.0	0.078434	0.080415	0.15519E-03	0.14838E-03	0.0002099	0.000732
90	0.40	0.30E 07	246.0	11.0	85.5	2196.0	435.2	0.078438	0.080411	0.15517E-03	0.14838E-03	0.0002143	0.000716
91	0.80	0.40E 07	230.0	6.5	95.5	3651.0	316.8	0.138750	0.140680	0.83372E-04	0.81335E-04	0.0001434	0.000806
92	0.80	0.40E 07	230.0	7.0	89.8	3651.0	317.0	0.138740	0.140680	0.83379E-04	0.81337E-04	0.0001489	0.000776
93	0.80	0.40E 07	230.0	7.5	85.5	3651.0	317.1	0.138740	0.140670	0.83380E-04	0.81339E-04	0.0001535	0.000750
94	0.80	0.40E 07	230.0	8.0	82.7	3651.0	317.2	0.138740	0.140670	0.83380E-04	0.81341E-04	0.0001589	0.000726
95	0.80	0.40E 07	230.0	8.5	78.4	3651.0	317.4	0.138740	0.140660	0.83377E-04	0.81342E-04	0.0001638	0.000704
96	0.40	0.25E 07	396.0	4.0	230.9	3536.0	564.6	0.074434	0.076239	0.24032E-03	0.23074E-03	0.0001420	0.001302
97	0.40	0.25E 07	396.0	4.5	222.4	3536.0	564.9	0.074428	0.076232	0.24034E-03	0.23076E-03	0.0001508	0.001224
98	0.40	0.25E 07	396.0	5.0	213.8	3536.0	565.2	0.074420	0.076226	0.24036E-03	0.23077E-03	0.0001587	0.001160
99	0.40	0.25E 07	396.0	5.5	203.9	3536.0	565.5	0.074407	0.076220	0.24042E-03	0.23078E-03	0.0001662	0.001106
100	0.40	0.25E 07	396.0	6.0	196.7	3536.0	565.7	0.074401	0.076215	0.24043E-03	0.23080E-03	0.0001738	0.001058
101	0.40	0.25E 07	396.0	6.5	185.6	3536.0	566.0	0.074400	0.076210	0.24042E-03	0.23081E-03	0.0001808	0.001016
102	0.40	0.25E 07	396.0	7.0	181.1	3536.0	566.2	0.074398	0.076205	0.24042E-03	0.23082E-03	0.0001878	0.000978
103	0.70	0.40E 07	538.0	6.5	219.5	1569.0	737.6	0.056558	0.060937	0.21574E-03	0.18867E-03	0.0001425	0.000802
104	0.70	0.40E 07	538.0	7.0	211.0	1569.0	738.0	0.056545	0.060926	0.21578E-03	0.18869E-03	0.0001478	0.000772
105	0.70	0.40E 07	538.0	7.5	205.3	1569.0	738.3	0.056532	0.060915	0.21583E-03	0.18872E-03	0.0001530	0.000744
106	0.70	0.40E 07	538.0	8.0	199.6	1569.0	738.5	0.056518	0.060905	0.21589E-03	0.18874E-03	0.0001579	0.000722
107	0.70	0.40E 07	538.0	8.5	195.3	1569.0	738.8	0.056504	0.060895	0.21594E-03	0.18876E-03	0.0001628	0.000700
108	0.80	0.40E 07	617.0	5.5	307.9	1377.0	842.4	0.048737	0.053626	0.25553E-03	0.21520E-03	0.0001310	0.000870
109	0.80	0.40E 07	617.0	6.0	296.5	1377.0	842.8	0.048714	0.053611	0.25567E-03	0.21524E-03	0.0001368	0.000830
110	0.80	0.40E 07	617.0	6.5	286.5	1377.0	843.1	0.048698	0.053598	0.25575E-03	0.21527E-03	0.0001423	0.000798
111	0.80	0.40E 07	617.0	7.0	278.0	1377.0	843.4	0.048686	0.053586	0.25580E-03	0.21531E-03	0.0001477	0.000770
112	0.80	0.40E 07	617.0	7.5	269.4	1377.0	843.7	0.048672	0.053574	0.25587E-03	0.21534E-03	0.0001527	0.000744
113	0.80	0.40E 07	617.0	8.0	262.3	1377.0	844.0	0.048656	0.053562	0.25595E-03	0.21537E-03	0.0001575	0.000720
114	0.80	0.40E 07	605.0	7.0	222.4	1350.0	837.1	0.048462	0.053343	0.25397E-03	0.21371E-03	0.0001475	0.000770
115	0.80	0.40E 07	605.0	7.5	216.1	1350.0	837.4	0.048443	0.053331	0.25407E-03	0.21374E-03	0.0001527	0.000744
116	0.80	0.40E 07	605.0	8.0	212.4	1350.0	837.7	0.048428	0.053319	0.25414E-03	0.21377E-03	0.0001576	0.000720

POINT NO.	MINF	REET	QINF	X	DELTAP	PINF	UE	RHOW	RHOE	NUW	NUE	THETA	CF
117	0.80	0.40E 07	605.0	8.5	208.1	1350.0	838.0	0.048418	0.053208	0.25418E-03	0.21380E-03	0.0001623	0.000700
118	0.90	0.50E 07	761.0	4.5	416.3	1699.0	837.2	0.060800	0.066866	0.20315E-03	0.17121E-03	0.0001061	0.000860
119	0.90	0.50E 07	761.0	5.0	394.9	1699.0	837.7	0.060765	0.066845	0.20329E-03	0.17125E-03	0.0001118	0.000814
120	0.90	0.50E 07	761.0	5.5	373.5	1699.0	838.0	0.060737	0.066827	0.20340E-03	0.17128E-03	0.0001171	0.000778
121	0.90	0.50E 07	761.0	6.0	355.0	1699.0	838.4	0.060710	0.066809	0.20350E-03	0.17131E-03	0.0001223	0.000744
122	0.90	0.50E 07	761.0	6.5	336.4	1699.0	838.8	0.060691	0.066792	0.20356E-03	0.17134E-03	0.0001273	0.000714
123	0.80	0.30E 07	453.0	8.0	109.8	1011.0	837.3	0.036300	0.039973	0.33873E-03	0.28485E-03	0.0001821	0.000832
124	0.80	0.30E 07	453.0	8.5	106.9	1011.0	837.6	0.036285	0.039965	0.33885E-03	0.28489E-03	0.0001875	0.000808
125	0.80	0.30E 07	453.0	9.0	105.5	1011.0	837.8	0.036283	0.039957	0.33887E-03	0.28492E-03	0.0001929	0.000786
126	0.80	0.30E 07	453.0	9.5	102.6	1011.0	838.1	0.036276	0.039949	0.33891E-03	0.28496E-03	0.0001982	0.000764
127	0.80	0.30E 07	453.0	10.0	99.8	1011.0	838.4	0.036265	0.039941	0.33902E-03	0.28501E-03	0.0002035	0.000744
128	0.80	0.30E 07	453.0	10.5	96.9	1011.0	838.6	0.036259	0.039934	0.33906E-03	0.28504E-03	0.0002084	0.000728
129	0.90	0.30E 07	492.0	8.5	134.0	867.7	927.6	0.031438	0.035437	0.39065E-03	0.31507E-03	0.0001871	0.000806
130	0.90	0.30E 07	492.0	9.0	132.6	867.7	927.9	0.031427	0.035429	0.39078E-03	0.31512E-03	0.0001925	0.000784
131	0.90	0.30E 07	492.0	9.5	131.2	867.7	928.2	0.031415	0.035420	0.39095E-03	0.31518E-03	0.0001979	0.000762
132	0.90	0.30E 07	492.0	10.0	129.7	867.7	928.5	0.031406	0.035411	0.39103E-03	0.31523E-03	0.0002032	0.000742
133	0.90	0.30E 07	492.0	10.5	128.3	867.7	928.8	0.031400	0.035404	0.39108E-03	0.31527E-03	0.0002078	0.000724
134	0.90	0.30E 07	492.0	11.0	128.3	867.7	929.0	0.031390	0.035397	0.39120E-03	0.31532E-03	0.0002127	0.000708
135	0.90	0.30E 07	492.0	11.5	128.3	867.7	929.3	0.031382	0.035388	0.39130E-03	0.31537E-03	0.0002175	0.000692
136	0.90	0.50E 07	842.0	5.0	399.2	1485.0	934.4	0.052921	0.059550	0.23565E-03	0.19066E-03	0.0001115	0.000812
137	0.90	0.50E 07	842.0	5.5	373.5	1485.0	934.9	0.052884	0.059530	0.23585E-03	0.19071E-03	0.0001168	0.000774
138	0.90	0.50E 07	842.0	6.0	355.0	1485.0	935.3	0.052855	0.059511	0.23600E-03	0.19075E-03	0.0001219	0.000742
139	0.90	0.50E 07	842.0	6.5	335.0	1485.0	935.7	0.052836	0.059492	0.23607E-03	0.19079E-03	0.0001269	0.000712
140	0.95	0.40E 07	691.0	4.0	365.0	1097.0	973.8	0.039560	0.045095	0.31274E-03	0.24830E-03	0.0001119	0.001016
141	0.95	0.40E 07	691.0	4.5	340.7	1097.0	974.3	0.039521	0.045075	0.31313E-03	0.24837E-03	0.0001184	0.000956
142	0.95	0.40E 07	691.0	5.0	322.2	1097.0	974.8	0.039583	0.045056	0.31353E-03	0.24844E-03	0.0001247	0.000908
143	0.95	0.40E 07	691.0	5.5	305.1	1097.0	975.2	0.039551	0.045040	0.31386E-03	0.24851E-03	0.0001305	0.000866
144	0.95	0.40E 07	691.0	6.0	290.8	1097.0	975.6	0.039523	0.045024	0.31413E-03	0.24856E-03	0.0001362	0.000828
145	0.95	0.40E 07	691.0	6.5	279.4	1097.0	976.0	0.039498	0.045008	0.31440E-03	0.24862E-03	0.0001420	0.000794
146	0.95	0.40E 07	691.0	7.0	270.5	1097.0	976.4	0.039478	0.044995	0.31454E-03	0.24866E-03	0.0001472	0.000766
147	0.95	0.40E 07	691.0	7.5	262.3	1097.0	976.7	0.039463	0.044981	0.31465E-03	0.24873E-03	0.0001525	0.000740
148	0.95	0.40E 07	691.0	8.0	253.8	1097.0	977.1	0.039447	0.044969	0.31479E-03	0.24877E-03	0.0001571	0.000718
149	0.95	0.40E 07	691.0	8.5	243.8	1097.0	977.4	0.039431	0.044957	0.31492E-03	0.24882E-03	0.0001619	0.000696
150	0.95	0.50E 07	873.0	5.0	394.9	1382.0	977.9	0.049563	0.056415	0.25149E-03	0.19934E-03	0.0001115	0.000810
151	0.95	0.50E 07	873.0	5.5	369.2	1382.0	978.3	0.049526	0.056394	0.25172E-03	0.19939E-03	0.0001168	0.000774
152	0.95	0.50E 07	873.0	6.0	349.3	1382.0	978.7	0.049490	0.056374	0.25195E-03	0.19944E-03	0.0001219	0.000740
153	0.95	0.50E 07	873.0	6.5	330.7	1382.0	979.1	0.049467	0.056356	0.25207E-03	0.19949E-03	0.0001267	0.000712

APPENDIX F

LISTING OF THE EXTENDED WU AND LOCK PROGRAM WITH AN EXAMPLE RUN

```
C
C
C
C     EXTENDED WU & LOCK PROGRAM.
C
C
C     MAIN PROGRAM ( ORIGINAL WU AND LOCK PROGRAM SLIGHTLY MODIFIED ).
C     ****************************************************************
C
C
C     THIS PROGRAM CALCULATES THE PRESSURE COEFFICIENT OVER A CONE IN
C     TRANSONIC FLOW AT AN ANGLE OF ATTACK, FOR WHICH SHOCK IS DETACHED.
C     INPUT PARAMETERS ARE EXPLAINED INSIDE THE PROGRAM.
C
      REAL MINF,KSIS,MAX                                              CO C00010
      COMMON /MSTR/ PT,GAMMA,GA1,GA2,GCMM                             00 000013
      COMMON /INF/ PINF,TINF,VINF                                     00 000015
      COMMON /SUB/ PTOT,P(125),V(125),X(125),ZM(125)                  00 C00016
      COMMON /PARM/ NPT,ISTART,MAXIT,TOL,TTOT,XL,IPASS,DELTA          00 000017
      DOUBLE PRECISION TARIKH                                         CO C00018
      DIMENSION Z(125),F(125),FN(125),D(125),Y(125),CP(125),          00 C00020
     1U(125),SE(125),SF(125),FN3(125),COI(125),                       00 C00025
     2AL(125),BL(125),CL(125),DL(125),EL(125),FL(125),SCL(125)        00 C00030
      DIMENSION TITLE(20)                                             00 000033
      NAMELIST /GROUP1/ MINF,ALFA,BETA                                00 000037
      NAMELIST /GROUP2/ REFT,QINF                                     00 C00040
      READ (5,*) NPT,ISTART,MAXIT,TOL,TTOT,XL,IPASS,DELTA             00 C00042
C
C     MINF = FREE-STREAM MACH NUMBER,
C     DELTA = SEMI-VERTEX ANGLE OF CONE IN DEGREES,
C     BETA = YAW ANGLE IN DEGREES,
C     ALFA = ANGLE OF ATTACK IN DEGREES,
C     REFT = REYNOLDS NUMBER PER FOOT, AND
C     QINF = FREE-STREAM DYNAMIC PRESSURE.
C
      CALL DATE (TARIKH)                                              00 000043
      WRITE (6,30) TARIKH                                             00 C00044
30    FORMAT (//' DATE RUN : ',A8/)                                   00 000045
26    READ(5,770,END=20)TITLE                                         00 000046
770   FORMAT(20A4)                                                    00 C00047
      WRITE(6,780)TITLE                                               00 000048
      WRITE(7,770)TITLE                                               00 000049
780   FORMAT(1X,20A4/)                                                00 C00050
      READ (5,GROUP1)                                                 00 000060
C
      THIRD=1./3.                                                     00 C00070
```

```
      GAMMA=1.4                                                          00 000080
      GA1=GAMMA-1.0                                                      00 000090
      GAM1=GAMMA+1.0                                                     00 000100
      GA2=GAMMA/GA1                                                      00 000110
      ZERO=0.0                                                           00 000120
      C1=-1.5                                                            00 000130
      C2=1.0                                                             00 000140
      C3=-0.25                                                           00 000150
C                                                                        00 000160
      WRITE(6,24)ALFA,BETA
7     CALL ANGLES(ALFA,BETA,THETA)                                       00 000190
C                                                                        00 000230

C     THETA = AZIMUTH ANGLE IN DEGREES.
C
9     ALFA=ABS(ALFA)/57.29578
      TETA=THETA/57.29578                                                00 000240
119   BE=1.0-MINF**2                                                     00 000250
      WRITE(6,625)MINF,DELTA,GAMMA                                       00 000260
      DEL=DELTA/57.29578                                                 00 000270
      GAM=GAM1*MINF**2                                                   00 000280
      SCTG=-2.0*SIN(ALFA)*COS(TETA)*DEL*GAM                              00 000290
      PT=(1.0+0.5*GAI*MINF**2)                                           00 000300
      IYE=0                                                              00 000310
C                                                                        00 000320
      IF(BE+GAM)2,3,3
2     WRITE(6,25)                                                        00 000330
      GO TO 20                                                           00 000340
C                                                                        00 000350
3     BB=SQRT(BE+GAM)
      GAMT=0.5*GAM*DEL**2                                                00 000360
      A=0.0                                                              00 000370
      H=0.01                                                             00 000380
      G(1)=0.0                                                           00 000390
      G(NPT)=0.0                                                         00 000400
      F(1)=BB                                                            00 000410
      F(NPT)=0.0                                                         00 000420
      FN(1)=BB                                                           00 000430
      FN(NPT)=0.0                                                        00 000440
      U(1)=-1.0                                                          00 000450
      U(NPT)=BE/GAM                                                      00 000460
      X(1)=0.0                                                           00 000470
      X(NPT)=1.0                                                         00 000480
      Y(1)=0.0                                                           00 000490
      Y(NPT)=1.0                                                         00 000500
C                                                                        00 000510
```

```
C     FIRST ITERATION :
C
      KSIS=4./BB                                                    00 000520
C
      NPI=NPT-1                                                     00 000525
      DO 4 I=2,NPI                                                  00 000530
      A=A+.01                                                       00 000540
      X(I)=BB*A*KSIS*(1.+A*(C1+A*(C2+C3*A)))                        00 000550
      F(I)=BB*(1.-A)**3                                             00 000560
      Y(I)=A                                                        00 000570
      FN3(I)=0.0                                                    00 000580
4     CONTINUE                                                      00 000590
C
5     A=0.0                                                         00 000600
      MAX=0.0                                                       00 000610
      ITE=ITE+1                                                     00 000620
C
      DO 9 I=2,NPI                                                  00 000630
      AA=-0.01                                                      00 000640
C
      DO 6 J=1,NPT                                                  00 000650
      AA=AA+H                                                       00 000660
      SE(J)=F(J)/SQRT((Y(I)-AA)**2+(X(I)*DEL/KSIS)**2)              00 000670
6     CONTINUE                                                      00 000680
C

      CALL SEKIBI(H,SE,Z,NPT)                                       00 000690
      FN(I)=0.0                                                     00 000700
      FINK=Z(NPT)*GAMT+BE*F(I)+SCTG*F(I)                            00 000710
      IF(FINK.GT.0.0)FN(I)=FINK**THIRD                              00 000720
      IF(FN(I).LT.0.0)FN(I)=F(I)*0.5                                00 000730
      D(I)=FN(I)-F(I)                                               00 000740
      U(I)=(BE-(FN(I))**2)/GAM                                      00 000750
5     CONTINUE                                                      00 000760
C
C

      CALL SEKIBI(H,FN,Z,NPT)                                       00 000770
      KSIS=1./Z(NPT)                                                00 000780
C
      DO 11 I=2,NPI                                                 00 000790
      CALL SEKIBI(H,FN,Z,I)                                         00 000800
      X(I)=KSIS*Z(I)                                                00 000810
11    CONTINUE                                                      00 000820
C
      DO 16 I=1,NPT                                                 00 00083
      BARF=ABS(D(I))                                                00 000840
```

```
      MAX=AMAX1(MAX,BARF)                                                  CO C00850
      F(I)=FN(I)                                                           CO C00860
16    CONTINUE                                                             CO C00870
C
      IF(MAX-.005)18,18,17                                                 CO C00880
17    IF(ITE-1015,2,2                                                      CO C00890
18    CONTINUE                                                             CO C00900
C
C
      ITER=0                                                               CO C00910
C
70    DO 71 I=2,NP1                                                        CO C00920
      AL(I)=(BE+SCTG)*F(I)                                                 CO C00930
      BL(I)=2.*F(I)*ALOG((.5*DEL*X(I)/KSIS)/SQRT(Y(I)*(1.-Y(I))))         CO C00940
      CL(I)=(1.-2.*Y(I))*X(I)/(KSIS*Y(I)*(1.-Y(I)))                        CO C00950
      EL(I)=X(I)/(KSIS*Y(I))                                               CO C00960
      FL(I)=(1.-X(I))/(KSIS*(1.-Y(I)))                                     CO C00970
71    CONTINUE                                                             CO C00980
C
      H=.01                                                                CO C00990
      IT=0                                                                 CO C01000
C
C
C
      DO 74 I=2,NP1                                                        CO C01010
C
      DO 75 J=1,NPT                                                        CO C01020
      IF(ABS(Y(J)-Y(I))77,76,77                                            CO C01030
76    SCL(J)=0                                                             CO C01040
      GO TO 78                                                             CO C01050
77    SCL(J)=(F(I)-F(J))/ABS(Y(J)-Y(I))                                    CO C01060
78    CONTINUE                                                             CO C01070
75    CONTINUE                                                             CO C01080
C
      CALL SEKIBI(H,SCL,Z,NPT)                                             CO C01090
      DL(I)=Z(NPT)                                                         CO C01100
      IF(IT)107,210,107                                                    CO C01110
210   CONTINUE                                                             CO C01120
C
      FN3(I)=AL(I)+1.5*DEL**2*GAM)*(-BL(I)+CL(I)-DL(I)-EL(I)-FL(I))        CO C01130
      IF(FN3(I).GT.0.0)FN(I)=FN3(I)**THIRD                                 CO C01140
      IF(FN3(I))107,107,106                                                CO C01150
107   FN(I)=FN(I-1)*.5                                                     CO C01160
      IT=IT+1                                                              CO C01170
106   CONTINUE                                                             CO C01180
      IF(FN3(I).LT.0.0)FN(I)=F(I)*.5                                       CO C01190
```

```
      D(I)*FN(I)-F(I)                                                    00 C01200
      U(I)=(BE-(FN(I))**2)/GAM                                           00 001210
74    CONTINUE                                                           00 C01220
C
C
      CALL SEKIB(H,FN,Z,NPT)                                             00 001230
      KSIS=1./Z(NPT)                                                     00 C01240
C
      DO 80 I=2,NP1                                                      00 C01250
      CALL SEKIB(H,FN,Z,I)                                               00 C01260
      X(I)=KSIS*Z(I)                                                     00 001270
80    CONTINUE                                                           00 001280
C
      ITER=ITER+1                                                        00 001290
C
      DO 81 I=1,NP1                                                      00 C01300
      F(I)=FN(I)                                                         00 001310
      CP(I)=-2.*U(I)-DEL**2*(1.-4.*(SIN(TETA))**2)*(SIN(ALFA))**2        00 001320
      PTL=(1.+.5*GAMMA*CP(I)*MINF**2)/PT**GA2                            00 C01330
      ZZ=(PTL**(-1./GA2)-1.)*2./GA1                                      00 C01340
      ZZ=AMAX1(ZZ,ZERO)                                                  00 C01350
      ZM(I)=SQRT(ZZ)                                                     00 C01360
81    CONTINUE                                                           00 C01370
C
      IF(ITER-3)70,301,301                                               00 C01380
301   CONTINUE                                                           00 C01390
      MAX=0.0                                                            00 C01400
      BAD=0.0                                                            00 C01410
C
      DO 101 I=2,NPT                                                     00 C01420
      IF(X(I)-.99)100,101,101                                            00 001430
100   BARF=ABS(D(I))                                                     00 001440
      DIF=CP(I)-CP(I-1)                                                  00 C01450
      IF(DIF.GE.0.0)BAD=1.0                                              00 C01460
      MAX=AMAX1(MAX,BARF)                                                00 C01470
101   CONTINUE                                                           00 C01480
C
      IF(MAX-.005)102,102,103                                            00 001490
103   IF(BAD-1.)102,104,104                                              00 C01500
104   IF(ITER-25)70,2,2                                                  00 001510
102   CONTINUE                                                           00 C01520
      ITER=ITE+ITER                                                      00 001530
C
      WRITE(6,26)ITER,KSIS                                               00 001540
C
```

```
      IF(ALFA)310,311,310                                              00 001550
311   DO 300 I=1,NPT                                                   CO C01560
      CDI(I)=CP(I)*X(I)*KSIS*FN(I)                                     00 001570
300   CONTINUE                                                         00 C01580
      CALL SEKIBI(H,CDI,Z,NPT)                                         00 C01590
      CD=2.*Z(NPT)                                                     CO 001600
C                                                                      00 001610
      WRITE(6,801)CD                                                   00 001620
310   CONTINUE
C                                                                      00 C01630
      GCMM=.5*GAMMA*MINF**2                                            00 001640
      HUNKY=.5/TAN(DEL)                                                CO C01650
      WRITE(6,227)                                                     00 001660
      DO 82 K=1,NPT                                                    00 C01670
      Q=X(K)*HUNKY                                                     CO C01680
      P(K)=CP(K)*GCMM+1.0                                              00 001700
      WRITE(6,228) K,X(K),CP(K),ZM(K),P(K),K                           00 001710
82    CONTINUE
C
C
24    FORMAT(//10X,'ANGLE OF ATTACK=',F10.3,5X,'ANGLE OF YAW=',F10.3,  00 001770
     2 '(DEGREES)'/)                                                   00 C01780
25     FORMAT(///10X,'SUPERSONIC FLOW : NO CONVERGENCE '///)           00 C01790
26    FORMAT(//20X,I2,'  ITERATIONS ',5X,'KSAI(SONIC) = ',F15.5/)      CO C01800
227   FORMAT(//25X,'X/L',T41,'CP',T57,'M',T70,'P/PINF'/)               00 C01810
228   FORMAT(I15,4F15.5,I10)                                           00 C01830
625   FORMAT(//20X,' MACH INF =',F8.4,5X,'CONE SEMI-VERTEX ANGLE ='    00 C01840
     4,F9.4,'(DEG)',5X,'GAMMA = ',F8.3/)                               00 C01850
801   FORMAT(// 10X,' DRAG COEFFICIENT = ',F13.5//)                    0C C01855
      IF (IPASS.EQ.2) GO TO 96                                         00 C01857
      READ (5,GROUP2)                                                  00 001860
      CALL DISI (MINF,REFT,QINF)                                       00 C01862
      IF ( IPASS.EQ.1 ) GO TO 95                                       00 C01863
      CALL INITIA                                                      00 001864
      WRITE (7,90)                                                     00 C01870
90    FORMAT(80('*'))                                                  00 C01872
96    WRITE(6,94)                                                      00 C01874
94    FORMAT(1H1)                                                      00 C01875
      GO TO 36                                                         00 C01877
20    STOP                                                             CO C01878
      END                                                              00 C01879
```

```
C
C
C
C       SUBROUTINE SEKIB
C       ****************
C
        SUBROUTINE SEKIB(H,W,Z,NDIM)                                    00001880
        DIMENSION W(125),Z(125)                                         00001890
        SUM2=0.0                                                        00001900
        DO 1 I=2,NDIM                                                   00001910
        SUM1=SUM2                                                       00001920
        SUM2=SUM2+.5*H*(W(I)+W(I-1))                                    00001930
1       Z(I-1)=SUM1                                                     00001940
        Z(NDIM)=SUM2                                                    00001950
2       RETURN                                                          00001960
        END                                                             00001970
```

```
C
C
C
C     SUBROUTINE ANGLES
C     ******************
C
C
C     THIS SUBPROGRAM CALCULATES THE EFFECTIVE ANGLE OF ATTACK AND THE
C     AZIMUTH ANGLE OF THE FLOW NEEDED IN THE MAIN PROGRAM.
C
      SUBROUTINE ANGLES(ALFA,BETA,THETA)                                00001980
      DOUBLE PRECISION DALFA,DALFAB,DBETA,DTHETA,X,Y,Z,RAD              00001982
      RAD=57.2957800                                                    00001988
      IF (BETA.NE.0.0) GO TO 2                                          00001992
      IF (ALFA.LT.0.0 ) GO TO 5                                         00001995
3     THETA=0.0                                                         00002000
      GO TO 4                                                           00002002
5     THETA = 180.0                                                     00002004
      GO TO 4                                                           00002006
C
2     DALFA=ALFA/RAD                                                    00002008
      DBETA=BETA/RAD                                                    00002015
      Y=DCOS(DBETA)*DTAN(DALFA)                                         00002018
      DTHETA=DATAN(Y)                                                   00002020
      X=DCOS(DBETA)*DCOS(DTHETA)                                        00002030
      DALFAB=DARCOS(X)                                                  00002040
      Z=Y/DTAN(DALFAB)                                                  00002050
      DTHETA=DARCOS(Z)                                                  00002060
      ALFAB=DALFAB*RAD                                                  00002070
C
C     ALFAB = EFFECTIVE ANGLE OF ATTACK.
C
      THETA=DTHETA*RAD                                                  00002080
      IF(ALFA.LT.0.0  )ALFAB=-ALFAB                                     00002090
      IF(BETA.LT.0.0  )THETA=-THETA                                     00002100
      ALFA=ALFAB                                                        00002120
4     CONTINUE                                                          00002125
C
      WRITE(6,1)ALFA,THETA                                              00002130
1     FORMAT(//10X,'EFFECTIVE ANGLE OF ATTACK =',F9.3 ,' DEGREES',      00002140
     $//10X,'AZIMUTH ANGLE =',F9.3 ,' DEGREES'//)                       00002150
      RETURN                                                            00002160
      END                                                               00002170
```

```
C
C
C
C     SUBROUTINE DIST
C     ***************
C
C     THIS SUBPROGRAM CALCULATES THE FREE-STREAM CONDITIONS AS WELL AS
C     THE VELOCITY DISTRIBUTION AT THE EDGE OF THE BOUNDARY LAYER TO BE
C     USED AS BOUNDARY CONDITIONS TO A BOUNDARY LAYER SOLVING PROGRAM.
C
      SUBROUTINE DIST (PINF,REFT,CINF)                                  00002180
      DIMENSION T(125)                                                  00002190
      COMMON /MSTR/ PT,GAMMA,GA1,GA2,GCNM                               00002200
      COMMON /SUB/ PTOT,P(125),V(125),X(125),ZM(125)                    00002205
      COMMON /INF/ PINF,TINF,VINF                                       00002207
      COMMON /PARM/ NPT,ISTART,XL,IPASS,DELTA                           00002209
C
C     ZM'S = LOCAL MACH NUMBERS.
C
      REAL MINF,MUINF                                                   00002210
C
C     MUINF = FREE-STREAM DYNAMIC VISCOSITY LBF S/FT**2.
C
      B=1.7973E+06                                                      00002220
      C=3.5694E+08                                                      00002230
      A=REFT*MINF/CINF                                                  00002240
      CONST=GAMMA*1716.C                                                00002260
      PTOT=CINF*PT**GA2/GCNM                                            00002270
C
C     PTOT = FREE-STREAM TOTAL PRESSURE PSF.
C
C
      TINF=(B+SQRT(B*B+4.C*A*C))/2.0/A                                  00002280
      TTOT=TINF*PT                                                      00002290
C
C     TINF = FREE-STREAM STATIC TEMPERATURE RANKIN.
C     TTOT = TOTAL TEMPERATURE.
C
      MUINF=2.27E-08*TINF*SQRT(TINF)/(TINF+198.6)                       00002320
      VINF=SQRT(CONST*TINF)*MINF                                        00002330
      PINF=PTOT/PT**GA2                                                 00002350
      RHOINF=PINF/53.35/TINF                                            00002360
C
```

```
      $)                                                                00002520
       WRITE(6,100) PINF,TINF,VINF,RHOINF,MUINF                         00002530
  100  FORMAT(5(5X,G10.4))                                              00002540
       DO 10 I=1,NPT                                                    00002550
       T(I)=TTOT/(1.0+0.5*GA1*ZM(I)**2)                                 00002560
       V(I)=ZM(I)*SQRT(GCNST*T(I))                                      00002570
C
C      T'S = LOCAL STATIC TEMPERATURES RANKIN.
C      V'S = EDGE VELOCITIES FT/S.
C
  10   CONTINUE                                                         00002580
       WRITE(6,93)                                                      00002590
  93   FORMAT(///45X,'VELOCITY DISTRIBUTION :' /)                       00002600
       WRITE(6,250)                                                     00002610
  250  FORMAT(// 51X,'M',13X,'X/L',13X,'U'/)                            00002620
       WRITE(6,200)(I,ZM(I),X(I),V(I),I=1,NPT)                          00002630
  200  FORMAT(35X,I5,5X,F10.5,5X,F10.5,5X,F10.2 )                       00002640
       RETURN                                                           00002650
  13   WRITE(6,300)                                                     00002660
  300  FORMAT(/5X,'MAX. ITERATIONS EXCEEDED'/)                          00002670
       RETURN                                                           00002680
       END                                                              00002690
C      VINF = FREE-STREAM VELOCITY.
C      RHOINF = FREE-STREAM DENSITY LBM/FT**3.
C      PINF = FREE-STREAM STATIC PRESSURE PSF.
C
       TTOT=TINF*PT                                                     00002410
       WRITE(6,150)                                                     00002420
  150  FORMAT(////7X,'MINF',12X,'RE/FT',11X,'QINF'/)                    00002430
       WRITE(6,110)MINF,REFT,QINF                                       00002440
  110  FORMAT(3(5X,G10.4))                                              00002450
       WRITE(6,160)                                                     00002460
  160  FORMAT(//5X,'PTOTAL',9X,'TTOTAL'/)                               00002470
       WRITE(6,120) PTOT,TTOT                                           00002480
  120  FORMAT(2(5X,G10.4))                                              00002490
       WRITE(6,170)                                                     00002500
  170  FORMAT(//6X,'PINF',11X,'TINF',11X,'UINF',12X,'RHOINF',10X,'MUINF'/00002510
```

```
C
C
C
C     SUBROUTINE INITIA
C     *****************
C
C
C
C     THIS SUBPROGRAM CALCULATES INITIAL VELOCITY AND TOTAL ENTHALPY
C     PROFILES IN THE BOUNDARY LAYER NEAR THE TIP OF THE CONE WHICH IS
C     NEEDED IN STAN-5 PROGRAM.
C
      SUBROUTINE INITIA                                                  00 002700
      COMMON /SUB/ PTOT,P(125),V(125),X(125),ZM(125)                     00 002710
      COMMON /INF/ PINF,TINF,VINF                                        00 002720
      COMMON /PARM/ NPT,ISTART,MAXIT,TOL,TTOT,XL,IPASS,DELTA             00 002725
      DIMENSION ETA(30),FPRIME(30),RW(125)                               00 002730
      REAL MIN,MUSTAR,NUSTAR                                             00 002740
      DATA PR/0.72/                                                      00 002750
C
C     BLASIUS SOLUTION.
C
      DATA ETA/0.0,0.1,0.2,0.3,0.4,0.5,0.6,0.7,0.8,0.9,1.0,1.1,1.2,1.3,  00 002752
     $1.4,1.5,1.6,1.7,1.8,1.9,2.0,2.2,2.4,2.6,2.8,3.0,3.4,3.8,4.2,5.0/   00 002753
      DATA FPRIME/0.0,0.04656,0.09391,0.14081,0.18761,0.23423,0.28058,   00 002755
     $0.32653,0.37196,0.41672,0.46063,0.50354,0.54525,0.58559,0.62439,   00 002756
     $0.66147,0.69670,0.72993,0.76106,0.79000,0.81669,0.86330,0.90107,   00 002757
     $0.93060,0.95288,0.96905,0.98797,0.99594,0.99862,1.0/               00 002758
      READ (5,*)  XLE                                                    00 002760
C
C     END OF LAMINAR PORTION, INCHES.
C
      XLE=XLE/12.0/XL                                                    00 002762
      IXLE=0                                                             00 002764
      IF ( XLE.LT.X(1) ) GO TO 67                                        00 002766
      DO 61 I=1,NPT                                                      00 002768
      IF((XLE.EQ.X(I)).OR.(XLE.GT.X(I).AND.XLE.LT.X(I+1)))GO TO 64       00 002770
61    CONTINUE                                                           00 002772
      IF ( IXLE.EQ.0 ) GO TO 67                                          00 002774
64    IXLE=I                                                             00 002776
      XIN=X(ISTART)*XL                                                   00 002780
      MIN=ZM(ISTART)                                                     00 002790
      UE=V(ISTART)                                                       00 002800
      R=SQRT(PR)                                                         00 002810
C
C     R = RECOVERY FACTOR, PR = PRANDTL NUMBER.
C
```

```
      T=TTOT/(1.0+0.2*MIN**2)                                          00002820
      TW=T*(1.0+R*0.2*MIN**2)                                          00002830
C
C     TW = WALL TEMPERATURE = ADIABATIC WALL TEMPERATURE APPROXIMATELY.
C
      TSTAR=T*(0.5+0.039*MIN**2+0.5*TW/T)                              00002840
      MUSTAR=2.27E-08*TSTAR*SQRT(TSTAR)/(TSTAR+198.6)                  00002850
C
C     THESE ARE THE AVERAGE TEMPERATURE AND DYNAMIC VISCOSITY ACROSS
C     THE BOUNDARY LAYER AT THE INITIAL LOCATION.
C
      PIN=P(ISTART)*PINF                                               00002860
C
C     INITIAL STATIC PRESSURE.
C
      WRITE(6,90)                                                      00002870
90    FORMAT(/8X,'TW',10X,'PINIT'/)                                    00002880
      WRITE(6,80) TW,PIN                                               00002890
80    FORMAT(5X,F8.2,6X,F8.2//)                                        00002900
      WRITE(7,70) PIN                                                  00002910
70    FORMAT(F10.2)                                                    00002920
      DO 60 I=ISTART,IXLE                                              00002930
      X(I)=X(I)*XL                                                     00002935
      RW(I)=X(I)*SIN(DELTA/57.29578)                                   00002940
C
C     RW'S ARE THE RADII OF THE CONE SURFACE AT THE VARIOUS X'S.
C
      WRITE(7,50) X(I),RW(I)                                           00002950
50    FORMAT(2(5X,F10.6))                                              00002960
60    CONTINUE                                                         00002970
      DO 40 I=ISTART,IXLE                                              00002980
      WRITE(7,30) V(I)                                                 00002990
30    FORMAT(5X,F10.2)                                                 00003000
C
C     THE EDGE VELOCITIES.
C
40    CONTINUE                                                         00003010
      RDSTAR=PIN/53.35/TSTAR                                           00003020
      NUSTAR=MUSTAR/RDSTAR*32.174                                      00003030
      YFACT=SQRT(3.0*UE/2.0/NUSTAR/XIN)                                00003040
      HFACT=50075.6/(1.0-R)                                            00003050
      HIN=0.24*TW                                                      00003060
      WRITE (6,100)                                                    00003063
100   FORMAT(' INITIAL PROFILE :'//10X,'Y',16X,'U',14X,'H'/)           00003065
      DO 20 I=1,30                                                     00003070
```

```
      Y=ETA(I)/YFACT                                                    00003080
      U=UE*FPRIME(I)                                                    00003090
      H=HIN+U**2/HFACT                                                  00003100
C
C     Y = THE NORMAL DISTANCE FROM CONE SURFACE IN FEET, U & H ARE THE
C     VELOCITY AND STAGNATION ENTHALPY PROFILES RESPECTIVELY.
C
      WRITE(6,10) Y,U,H                                                 00003110
      WRITE(7,10) Y,U,H                                                 00003120
10    FORMAT(5X,  E10.4,2(5X,F10.2))                                    00003130
20    CONTINUE                                                          00003140
      RETURN                                                            00003150
67    WRITE (6,69) XLE                                                  00003160
69    FORMAT(/5X,'ERROR IN XLE. VALUE READ =',2X,F8.5)                  00003170
      RETURN                                                            00003180
      END                                                               00003190
```

21	0.20436	0.04341	0.48853	1.00760	21
22	0.21448	0.04283	0.48868	1.00749	22
23	0.22460	0.04226	0.48883	1.00739	23
24	0.23471	0.04170	0.48898	1.00730	24
25	0.24483	0.04116	0.48913	1.00720	25
26	0.25494	0.04062	0.48927	1.00711	26
27	0.26505	0.04009	0.48941	1.00701	27
28	0.27517	0.03956	0.48955	1.00692	28
29	0.28528	0.03904	0.48969	1.00683	29
30	0.29539	0.03853	0.48982	1.00674	30
31	0.30549	0.03801	0.48996	1.00665	31
32	0.31560	0.03750	0.49009	1.00656	32
33	0.32571	0.03700	0.49023	1.00647	33
34	0.33581	0.03649	0.49037	1.00638	34
35	0.34592	0.03598	0.49050	1.00630	35
36	0.35602	0.03547	0.49063	1.00621	36
37	0.36612	0.03497	0.49077	1.00612	37
38	0.37622	0.03446	0.49091	1.00603	38
39	0.38632	0.03394	0.49104	1.00594	39
40	0.39642	0.03343	0.49118	1.00585	40
41	0.40652	0.03291	0.49131	1.00576	41
42	0.41662	0.03238	0.49145	1.00567	42
43	0.42671	0.03186	0.49160	1.00557	43
44	0.43681	0.03132	0.49174	1.00548	44
45	0.44690	0.03078	0.49188	1.00539	45
46	0.45700	0.03024	0.49202	1.00529	46
47	0.46709	0.02968	0.49217	1.00519	47
48	0.47718	0.02912	0.49232	1.00510	48
49	0.48727	0.02855	0.49247	1.00500	49
50	0.49736	0.02796	0.49263	1.00489	50
51	0.50744	0.02737	0.49278	1.00479	51
52	0.51753	0.02676	0.49294	1.00468	52
53	0.52761	0.02615	0.49311	1.00457	53
54	0.53770	0.02551	0.49328	1.00446	54
55	0.54778	0.02487	0.49344	1.00435	55
56	0.55786	0.02420	0.49362	1.00424	56
57	0.56794	0.02352	0.49380	1.00412	57
58	0.57802	0.02282	0.49399	1.00399	58
59	0.58809	0.02210	0.49418	1.00387	59
60	0.59817	0.02136	0.49437	1.00374	60
61	0.60824	0.02059	0.49457	1.00360	61
62	0.61832	0.01980	0.49479	1.00346	62
63	0.62839	0.01898	0.49500	1.00332	63
64	0.63846	0.01813	0.49522	1.00317	64
65	0.64852	0.01725	0.49546	1.00302	65
66	0.65859	0.01633	0.49570	1.00286	66

67	0.66865	0.01537	0.49595	1.00269	67
68	0.67871	0.01437	0.49622	1.00251	68
69	0.68877	0.01332	0.49649	1.00233	69
70	0.69883	0.01223	0.49678	1.00214	70
71	0.70889	0.01107	0.49708	1.00194	71
72	0.71894	0.00986	0.49741	1.00172	72
73	0.72899	0.00857	0.49775	1.00150	73
74	0.73904	0.00721	0.49810	1.00126	74
75	0.74908	0.00576	0.49848	1.00101	75
76	0.75912	0.00422	0.49889	1.00074	76
77	0.76916	0.00258	0.49932	1.00045	77
78	0.77920	0.00081	0.49979	1.00014	78
79	0.78923	-0.00109	0.50028	0.99981	79
80	0.79926	-0.00315	0.50082	0.99945	80
81	0.80928	-0.00538	0.50141	0.99906	81
82	0.81930	-0.00782	0.50205	0.99863	82
83	0.82931	-0.01050	0.50275	0.99816	83
84	0.83932	-0.01345	0.50352	0.99765	84
85	0.84932	-0.01674	0.50438	0.99707	85
86	0.85932	-0.02042	0.50534	0.99643	86
87	0.86931	-0.02459	0.50643	0.99570	87
88	0.87928	-0.02934	0.50766	0.99487	88
89	0.88925	-0.03482	0.50909	0.99391	89
90	0.89921	-0.04124	0.51076	0.99278	90
91	0.90915	-0.04886	0.51273	0.99145	91
92	0.91907	-0.05810	0.51512	0.98983	92
93	0.92898	-0.06955	0.51807	0.98783	93
94	0.93885	-0.08416	0.52182	0.98527	94
95	0.94870	-0.10352	0.52677	0.98188	95
96	0.95849	-0.13054	0.53364	0.97716	96
97	0.96822	-0.17107	0.54386	0.97006	97
98	0.97783	-0.23915	0.56082	0.95815	98
99	0.98722	-0.37904	0.59455	0.93367	99
100	0.99592	-0.84974	0.70507	0.85130	100
101	1.00000	-2.50762	1.09189	0.56117	101

MINF	RE/FT	QINF
.5000	.4000E+07	404.0

PTOTAL	TTOTAL
2738.	530.8

PINF	TINF	UINF	RHOINF	MUINF
2309.	505.5	551.1	.8559E-01	.3666E-06

VELOCITY DISTRIBUTION :

	M	X/L	U
1	0.0	0.0	0.0
2	0.48140	0.01181	531.45
3	0.48255	0.02197	533.13
4	0.48389	0.03213	534.08
5	0.48452	0.04228	534.75
6	0.48502	0.05242	535.27
7	0.48543	0.06257	535.70
8	0.48578	0.07271	536.07
9	0.48609	0.08284	536.40
10	0.48637	0.09298	536.70
11	0.48663	0.10311	536.97
12	0.48687	0.11325	537.22
13	0.48709	0.12338	537.45
14	0.48730	0.13350	537.67
15	0.48749	0.14363	537.88
16	0.48769	0.15376	538.08
17	0.48787	0.16388	538.27
18	0.48804	0.17400	538.45

19	0.48820	0.18412	538.62
20	0.48831	0.19424	538.80
21	0.48853	0.20436	538.96
22	0.48868	0.21448	539.13
23	0.48883	0.22460	539.29
24	0.48898	0.23471	539.44
25	0.48913	0.24483	539.60
26	0.48927	0.25494	539.74
27	0.48941	0.26505	539.89
28	0.48955	0.27517	540.04
29	0.48969	0.28528	540.19
30	0.48982	0.29539	540.33
31	0.48994	0.30545	540.47
32	0.49009	0.31560	540.62
33	0.49023	0.32571	540.76
34	0.49037	0.33581	540.90
35	0.49050	0.34592	541.04
36	0.49063	0.35602	541.18
37	0.49077	0.36612	541.33
38	0.49091	0.37622	541.47
39	0.49104	0.38632	541.61
40	0.49118	0.39642	541.76
41	0.49131	0.40652	541.90
42	0.49145	0.41662	542.05
43	0.49160	0.42671	542.20
44	0.49174	0.43681	542.34
45	0.49188	0.44690	542.49
46	0.49202	0.45700	542.64
47	0.49217	0.46709	542.80
48	0.49232	0.47718	542.95
49	0.49247	0.48727	543.12
50	0.49263	0.49736	543.28
51	0.49278	0.50744	543.44
52	0.49294	0.51753	543.61
53	0.49311	0.52761	543.78
54	0.49328	0.53770	543.96
55	0.49344	0.54778	544.14
56	0.49362	0.55786	544.32
57	0.49380	0.56794	544.52
58	0.49399	0.57802	544.71
59	0.49418	0.58809	544.91
60	0.49437	0.59817	545.11
61	0.49457	0.60824	545.33
62	0.49479	0.61832	545.55
63	0.49500	0.62839	545.77
64	0.49522	0.63846	546.01

65	0.49546	0.64852	546.25
66	0.49570	0.65855	546.51
67	0.49595	0.66865	546.77
68	0.49622	0.67871	547.05
69	0.49649	0.68877	547.34
70	0.49678	0.69883	547.65
71	0.49708	0.70889	547.97
72	0.49741	0.71894	548.30
73	0.49775	0.72899	548.66
74	0.49810	0.73904	549.04
75	0.49848	0.74908	549.43
76	0.49889	0.75912	549.86
77	0.49932	0.76916	550.31
78	0.49979	0.77920	550.80
79	0.50028	0.78923	551.32
80	0.50082	0.79926	551.89
81	0.50141	0.80928	552.50
82	0.50205	0.81930	553.18
83	0.50275	0.82931	553.91
84	0.50352	0.83932	554.72
85	0.50438	0.84932	555.62
86	0.50534	0.85932	556.63
87	0.50642	0.86931	557.77
88	0.50766	0.87928	559.06
89	0.50909	0.88925	560.55
90	0.51076	0.89921	562.30
91	0.51273	0.90915	564.37
92	0.51512	0.91907	566.86
93	0.51807	0.92898	569.94
94	0.52182	0.93885	573.86
95	0.52677	0.94870	579.02
96	0.53364	0.95849	586.16
97	0.54386	0.96822	596.77
98	0.56082	0.97783	614.29
99	0.59495	0.98722	649.27
100	0.70507	0.99592	759.36
101	1.09189	1.00000	1105.00

Tw	PINIT
527.24	2334.45

INITIAL PROFILE :

Y	U	H
0.0	0.0	126.54
0.1212E-04	25.04	126.54
0.2424E-04	50.07	126.54
0.3636E-04	75.07	126.55
0.4848E-04	100.02	126.57
0.6060E-04	124.87	126.58
0.7272E-04	149.59	126.60
0.8484E-04	174.08	126.63
0.9696E-04	198.30	126.66
0.1091E-03	222.17	126.69
0.1212E-03	245.58	126.72
0.1333E-03	268.45	126.76
0.1454E-03	290.69	126.79
0.1576E-03	312.20	126.83
0.1697E-03	332.88	126.87
0.1818E-03	352.65	126.91
0.1939E-03	371.43	126.95
0.2060E-03	389.15	127.00
0.2182E-03	405.74	127.04
0.2303E-03	421.17	127.07
0.2424E-03	435.40	127.11
0.2656E-03	460.25	127.18
0.2939E-03	480.39	127.24
0.3151E-03	496.13	127.28
0.3393E-03	508.01	127.32
0.3636E-03	516.63	127.34
0.4121E-03	526.72	127.38
0.4605E-03	530.97	127.39
0.5090E-03	532.50	127.39
0.5090E-03	533.13	127.40